Master Thesis
TVVR 19/5001

Present and Future Extreme Weather in Sweden According to the d4PDF

Dennis Davour

Division of Water Resources Engineering
Department of Building and Environmental Technology
Lund University

Present and Future Extreme Weather in Sweden According to the d4PDF

By:
Dennis Davour

Master Thesis

Division of Water Resources Engineering
Department of Building & Environmental Technology

Lund University
Box 118
221 00 Lund, Sweden

Water Resources Engineering
TVVR-19/5001
ISSN 1101-9824

Lund 2019
www.tvrl.lth.se

Master Thesis
Division of Water Resources Engineering
Department of Building & Environmental Technology
Lund University

Swedish title: Nutida och framtida extremväder i Sverige enligt d4PDF
English title: Present and Future Extreme Weather in Sweden According to the d4PDF
Author(s): Dennis Davour
Supervisor: Ronny Berndtsson, Noriaki Hashimoto, Masaru Yamashiro
Examiner: Magnus Larson
Language English
Year: 2019
Keywords: Climate change; extreme weather; climate database; statistical analysis; RCP8.5

Acknowledgements

I would like to take this opportunity to express my gratitude and appreciation towards both Kyushu University and Lund University for the opportunity to participate in the double degree exchange program. My time in Fukuoka and at Kyushu University has been incredibly valuable and I will appreciate my experiences here eternally. Also thank you both for your support through the Kyushu University Friendship Scholarship and the EU-JAMM scholarship – it has made the time here that much more enjoyable and has given me the opportunity for many additional cultural experiences.

I would especially like thank my professors and supervisors in the Coastal and Ocean Engineering Laboratory, Prof. Noriaki Hashimoto and Prof. Masaru Yamashiro. Also, sincere thanks to Yoshihiko Ide, Kodama Mitsuyoshi, Md Abdul Al Mohit, Naoyuki Nakao and Taiki Shibata for your support and input during my time here.

Lastly, I am extremely grateful to all the members of my Laboratory and friends at Kyushu University and in Fukuoka City for your warm welcome and friendship. My stay here would not have been half as enjoyable if I hadn't met you all.

Once again,
A sincere, thank you all

Abstract

Natural events that happen more rarely have historically been more difficult to study and continue to require different methods. For example, rare occurrences of natural disasters and weather events can have return periods of thousands of years but because of their large impact are very important to study. In addition to being used to study the changing climate, climate models have the advantage of being able to produce large amounts of climate data. This is taken advantage of by the climate data database d4PDF which is especially customized for extreme weather analysis through having 6000 years of data in both the present and end-of-century climate in the RCP8.5 development scenario. Additionally, the future climate parameters are chosen in order to disregard the climate change during the simulated period. The d4PDF data for Sweden was validated for the general temperature and precipitation climate and found to match well with observation data and other climate change simulations. The temperature and precipitation increases the most in the North and during the winter season. Moreover, it was found that the maximum daily temperature of the year increases in general quite evenly – except for in the South-East where the increase for long return period events is higher. For precipitation events it was found that the precipitation increases most for short duration events and that it increases more for events with longer return periods.

Table of contents

1 Introduction

Earth's history stretches further back than what can truly be comprehended. The period that humans have lived on the surface is but a tiny percentage and civilization but a fraction of that. Directly after the formation of Earth climate change began and over the billions of years it was made habitable by life. Life and climate change have since then formed a peculiar relationship where life adapts to the climate around it, populating the most inaccessible places, and life affecting the surrounding climate to various degrees. One considerable change is the release of oxygen where early life released, the to them harmful, oxygen to the atmosphere forming the basis for the conditions we still know today.

The most recent acknowledged geologic epoch is the Holocene where the Earth's climate has been kept quite warm and unusually stable for approximately the past 12,000 years. This period coincides with the formation of human civilizations around the Earth and because civilization's immense impact on Earth it has been suggested that we are leaving the Holocene for the Anthropocene. The Anthropocene is defined as having humans as the most recognizable force for change on Earth instead of more fundamental processes. It has been concluded that it is now extremely likely that humans are the main cause of the current global warming and even though climate change is a natural event, and even naturally affected by life forms, it could serve our best interests to instead try to keep the climate as favorable and stable as possible.

1.1 Climate Change

The IPCC was founded in 1988 and has since released 5 assessment reports (ARs) on climate change. The most recent AR5 was released in stages in 2013-2014 and it consisted of three working groups (WG) that produced one report each:

- WG I: The Physical Science Basis
- WG II: Impacts, Adaptation and Vulnerability
- WG III: Mitigation of Climate Change

In AR5 it is confirmed that the human influence on the climate system is growing and that it is extremely likely that humans are the main cause of the current global warming. The observed changes since the 1950s are unprecedented and the larger the disruption, the greater the risk for severe impacts on ecosystems around the Earth.

The key driving force for future climate change is the release of greenhouse gases (GHGes) where there is a strong, almost linear, relationship between cumulative anthropogenic GHG emissions and temperature change relative to pre-industrial levels. Therefore, to research the future climate it is fundamental to determine different scenarios for the future GHG emissions. Four scenarios for the development of human society during the 21st century was constructed called the Representative Concentration Pathways (RCPs). These scenarios range between very strict mitigation (RCP2.6) and a continued increase in emissions (RCP8.5). (IPCC, 2014b)

1.2 General Circulation Model

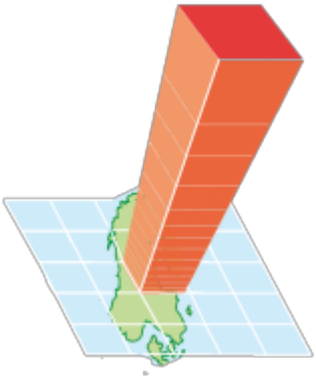

Figure 1.1: The principle of climate models where the land surface is separated into a grid and the atmosphere is represented by several grids stacked - forming boxes. (SMHI, 2009a)

Once there are tools to represent the future driving force behind climate change (the RCPs) the next step is how to determine the effect the GHGes have on the climate. For this purpose, several climate models have been developed. Climate models are basically computer simulations of the Earth's atmosphere – and sometimes the hydrosphere or at least the world oceans. The climate is represented by a 3D-model where the surface is divided into a grid – much like longitude and latitude – and the atmosphere by several grids on top of each other – forming many boxes as seen in figure 1.1.

Once the 3D-space is constructed each point represents a land area or an air volume. These can then be assigned characteristics and how they would influence each other depending on these. These characteristics could for example be temperature, water content, air pressure, wind speed and direction.

The calculations require a lot of processing power and often the grid is quite large to decrease the number of points. Often General Circulation Models (GCMs) have a grid size of 100-300km which is not detailed enough to model differences in climate on a regional scale. Thus, Regional Circulation Model (RCMs) are often used to model the climate on smaller scales. The RCMs use the result from a GCM as input data, considering the changes on a global scale. This way the RCMs can generate more detailed data, often called downscaled data, in a smaller grid to help in regional studies without risking being detached from the global climate. (SMHI, 2009a)

As computer technology is improved the global models can use an increasingly smaller grid. During the first IPCC report in 1990 the typical resolution was about 500km. Since then, the resolution has improved and is typically now 100km. (Le Treut et al., 2007) However, there are outliers with resolutions of about 20km such as the MRI-AGCM3.2 models but then at the expense of other aspects in the model such as ocean simulations. (Mizuta et al., 2012)

To evaluate the performance, the most straightforward approach is to compare the model results to actual observed values. The models can be run both for past and future climate and if the past simulated climate is compared to observations and estimates the models accuracy can be determined. To further reduce the uncertainties when it comes to future simulated climate, ensembles of several climate models are used. Either several independent models are used to explore their variability, Multi-Model Ensembles (MMEs), or the same model is used but with a change in conditions, so called Perturbed-Parameter Ensembles (PPEs). Both MMEs and PPEs have their disadvantages. PPEs cannot explore the model's structural uncertainties. Instead they investigate the uncertainties from the parameters used when running the model. MMEs on the other hand have a much smaller sampling size and are further complicated by several models sharing certain parts of the model – and can thus not be considered truly independent. (Flato et al., 2013)

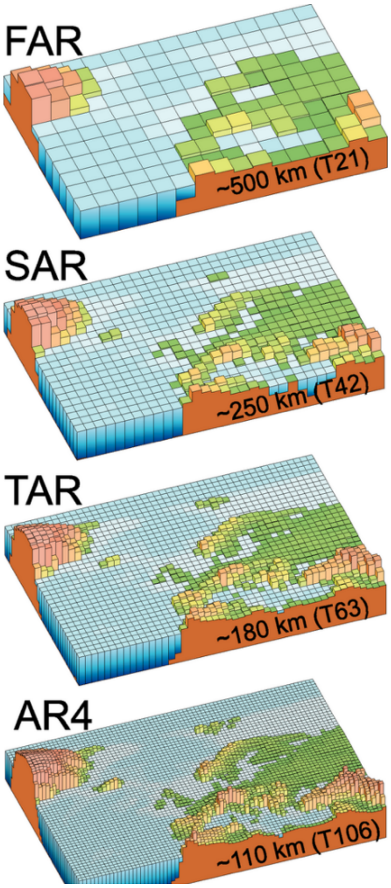

Figure 1.2: Representative resolution used in the short-term simulations made in the IPCC reports. FAR 1990, SAR 1996, TAR 2001, and AR4 2007. The long-term simulations in a report generally use the resolution of the previous report short-term simulation. (Le Treut et al., 2007)

1.2.1 Coupled Model Inter-comparison Project

The Coupled Model Inter-comparison Project (CMIP) is an initiative by the Working Group on Coupled Modelling (WGCM) and it began in 1995. Coupled models are GCMs with a coupled simulation of the ocean and atmosphere – Atmosphere-Ocean Coupled General Circulation Models (AOGCMs or CGCMs). The purpose of the project is to better understand changes in climate due to natural variability and anthropogenic activity using multiple models. Another objective is to make the multi-model output available in a standardized format. There have been several major experiments along with many smaller ones. (WRCP, n.d.)

The most recent major phase was CMIP phase 5 (CMIP5) which provided a standard for simulations in order to:

- evaluate how realistic the models are in simulating the recent past,
- provide projections of future climate change on two time scales, near term (out to about 2035) and long term (out to 2100 and beyond), and
- understand some of the factors responsible for differences in model projections, including quantifying some key feedbacks such as those involving clouds and the carbon cycle (Taylor, Stouffer, & Meehl, 2009)

Standardized accessible results are available to researchers worldwide which makes MME analysis significantly easier. The ensemble can then provide a representation of the overall estimations of the scenario outcomes using approximately independent models. The models used are the best attempts to simulate the climate system and the collective estimate provides a representation of the climate model consensus. Also, the spread in results from the models can be used as a measure of the reliability of the result. (Taylor et al., 2012)

1.3 Extreme weather

The most publicly discussed change in climate is the average temperature since it is quite simply related to the GHG concentration in the atmosphere. However, climate change affects the whole climate system which leads to changes not only in the average temperature. Examples of other changes are glaciers melting, sea-level rise and changes in vegetation. It is an intricate system requiring an understanding of feedback processes and interactions to create the GCMs.

The climate system also determines the properties of rare, extreme weather and climate events such as severe storms, droughts and heat waves. In a future climate there will be changes in the frequency, intensity and duration of extreme events but the changes could take different forms. For example, an increase in average temperature by 4°C would not necessarily mean that it is simply evenly warmer than before, illustrated in Figure 1.3 (a). The temperature could also change by having a greater variability (b), where what previously was extreme weather becomes more common. Also, there could be a change in the symmetry (c) causing the extremes on one side to become more common while the other stays the same. Changes in the properties of extreme events can be linked to one of these three changes of the distribution or to a combination of them. (IPCC, 2012)

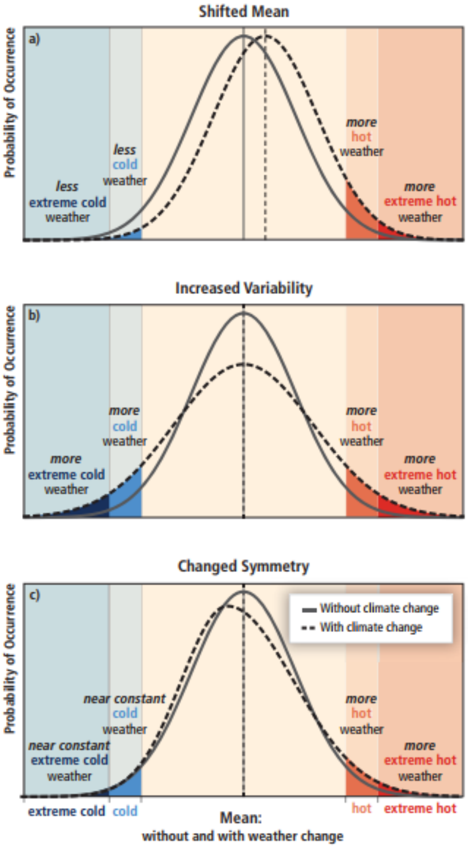

Figure 1.3: Different changes in temperature distribution and their effects on extreme values. (a) Effect of a shift in mean temperature. (b) Effects of an increase in variability/variance (c) Effects of a change in symmetry/shape of the distribution. (IPCC, 2012)

1.4 The geography and current climate in Sweden

Japan, having experienced the devastating effects of the 2011 Tohoku Earthquake, understand better than most the importance of studying low-frequency severe events. Disasters with extremely low probabilities of once in 1,000 years or less can still occur and when they do, they can cause massive damage to human lives and infrastructure. Besides from frequently being affected by Earthquakes, Japan also have a yearly rainy season and volcanoes. Combined all this makes Japan a rather disaster-prone country, but it has also given rise to a resilient people.

Sweden on the other hand is rather seldom affected by natural disasters. A speaking example is that the natural disaster where most Swedish people were killed was the severe earthquake and following Tsunami in the Indian Ocean in late 2004. Many Swedish people at the time had travelled to warmer latitudes for the winter holidays and 543 were unfortunately killed. Besides that, in Sweden, storms have claimed the most lives and caused the highest economic damage; roughly 100 people have been since 1967 and one severe storm in 2005 caused more than 20 billion SEK in damages (roughly 2.5 billion USD). (MSB, 2017) Compared to other countries these numbers could seem small, but Sweden only just passed a population of 10 million.

The reason why storms cause relatively much damage is in a large part because the important forestry industry. With 70% of the area covered mainly by coniferous forest it is one of Sweden's largest industries. The elongated country varies significantly from south to north. The north is sparsely populated with many mountains, forests and lakes. The many rivers flowing from west to north are commonly used to generate hydroelectric power. The southern regions of Sweden contain the 3 largest cities and has a lot of agriculture and farmland. There are about 1800 hydroelectric power plants in Sweden that generate almost half of the electricity needed. However, most of the production was constructed before 1975. Considering that the future climate could change the circumstances in water resources for the hydropower one should be cautious of the risk concerning the safety of older dams. Regarding the southern parts of the country the future risks are probably more related to the agriculture. Just last year, in the summer of 2017, Sweden had the worst water shortage in the south-east in 100 years after 2 years of unusually low precipitation.

In Sweden the Swedish Meteorological and Hydrological Institute (SMHI) is the expert agency under the Ministry of the Environment and Energy that is responsible for analyzing meteorology, hydrology, oceanography and climatology to strive for greater public welfare, increased safety and a sustainable society. They work with weather forecasts and warnings, professional services, research and development, observations and analysis and also climate data analyses and research. Climate observations started as far back as in the 1800s and has since then developed into a network with both manual and automatic observation stations. The future climate is being researched at the climate research unit Rossby Center. There are available results from a regional climate model, RCA4, for Sweden for the RCP4.5 and RCP8.5 scenarios that are summarized for the temperature and precipitation next.

1.4.1 Future temperature change in Sweden

The present yearly average temperature is represented by the normal annual mean temperature during 1961-1990. There temperature increases from south to north, with also the coast line being slightly warmer. The temperature is 6-8 degrees in the south and -4-0 in the north. (Figure 1.4)

Globally the increase in temperature until the end of the century is expected to be between 0.5 and 5 degrees, depending on the emissions scenario. (IPCC, 2014a) In Sweden the increase is expected to be slightly higher. The SMHI regional climate simulations for Sweden based on the RCP4.5 and RCP8.5 show that the temperature increases between 2 to 7 degrees by 2100 compared to 1961-1990. The winter season has the greatest temperature increase of 2 to 9 degrees with summer having an increase of 1 to 7 degrees. There are significant regional differences with the highest increase in north Sweden. (Klimatanpassningsportalen, 2013)

The effect of increasing temperatures is in part shifting vegetation zones. This introduces new species from the south but also moves the current vegetation zone north, possibly disturbing the important forestry industry. Also, this would raise the vertical tree line and thus changing the natural heritage in the northern mountainous areas, where there are no trees growing high up. The length of the growing season is expected to increase (the number of consecutive days with a daily average temperature above 5 degrees) by 1-2 months throughout Sweden, except for the far south where the increase would be 3 months. (Klimatanpassningsportalen, 2013)

1.4.2 Future precipitation change in Sweden

The present annual precipitation during the normal period 1961-1990 is quite even across the country. Mostly the precipitation is 500-700mm with higher levels on the south-west coast and in the north west mountains, 900-1200mm. (Figure 1.4) There is no rainy season in Sweden as opposed to Japan and the precipitation is quite evenly distributed over the year.

According to the SMHI regional simulations the precipitation in Sweden increases by 0-40% until 2100. The variations in precipitations are much larger than for the temperature, both between years and decades. The greatest increase occurs in winter. During the summer the precipitation decreases in southern Sweden while the increase is small in the north. This gives rise to a large range of possible developments in the future.

In winter the temperature increases results in a shorter snowy season with lower snow coverage, despite the higher amounts of precipitation. Still the water supply increases in Sweden except for in the south-east. There will be changes in the river flows annual patterns especially leading to more unstable winters with higher flows. (Klimatanpassningsportalen, 2016)

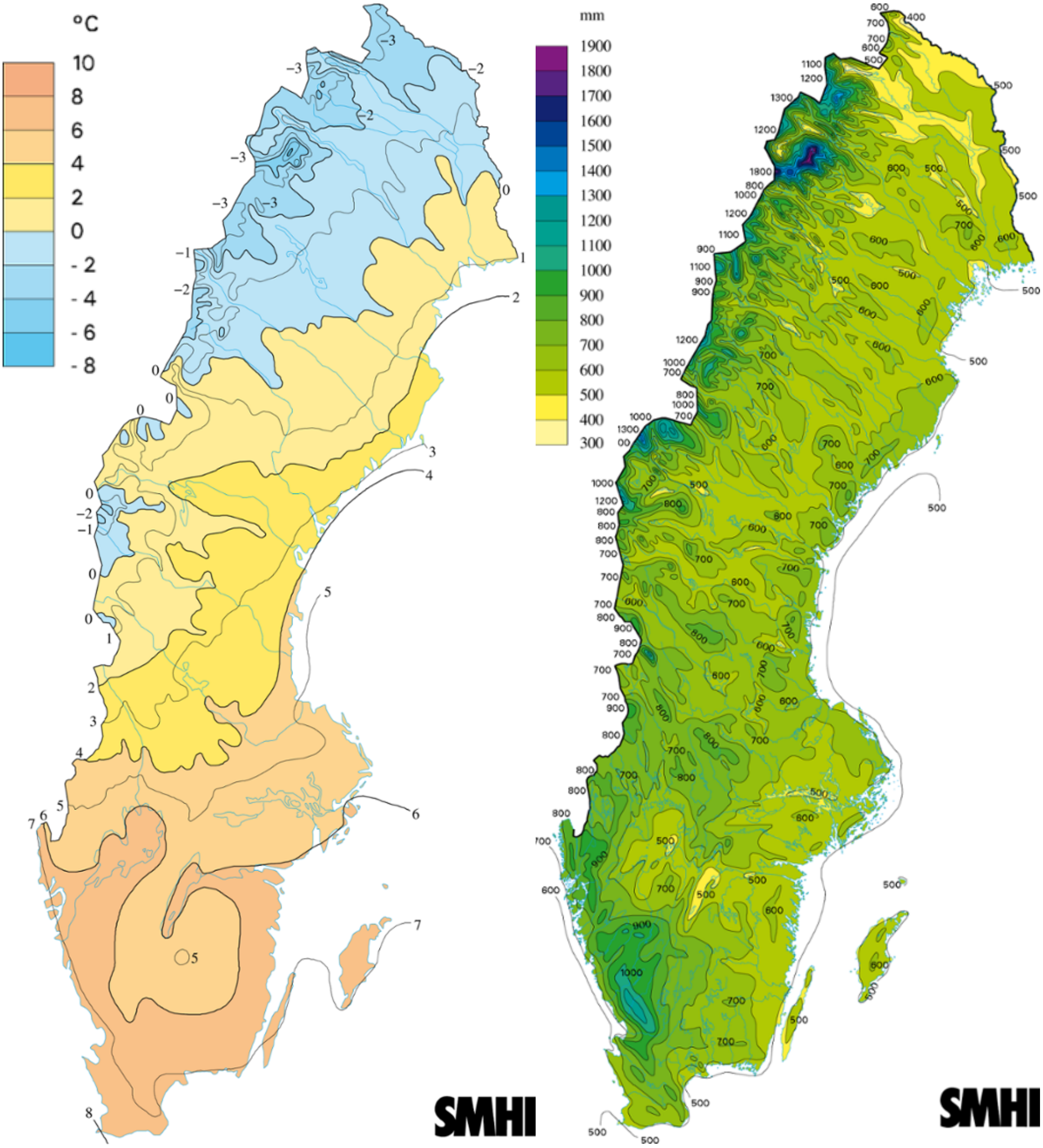

Figure 1.4: The yearly average temperature (left) and precipitation (right) in Sweden during 1961-1990. (SMHI, 2009b)

1.5 The aim of the study

The foremost addition of this study will be to add to the future extreme weather estimations for Sweden. In order to do this in a convincing way the model used must firstly, be considered accurate in predicting the general current climate. Secondly, the model should generate a similar estimate of the future climate as previously used and accepted climate models. Therefore, the result of this study will include the model's comparison to measurements to represent the present climate. For the future climate comparison, the main model ensemble used for climate change studies in Sweden under similar conditions will be used. The work is by choice limited to temperature and precipitation-related aspects of the climate and thus includes yearly maximum temperature, heat waves, maximum precipitation during various periods and droughts.

2 Methods

In this study the database for Policy Decision-making on Future climate change (d4PDF) was used to analyze extreme weather events. The result from the d4PDF was compared to measurements and climate ensemble results from the Swedish Meteorological and Hydrological Institute (SMHI).

The relevant part of the d4PDF was acquired from Japan Agency for Marine-Earth Science and Technology (JAMSTEC) by copying the relevant files (approximately 100TB) using a script through a secure SSL connection. The secure connection was established by Global Protect and thereafter the data transfer was handled via Tera Term with a shell script. Thereafter the relevant region was selected (50-70°N, 0-30°E) and the temperature and precipitation data (.grib format) extracted to ASCII using GrADS via a script. The resulting files were then handled in MATLAB in order to visualize and analyze the climate data mostly through the use of sorting the data into multi-dimensional matrices.

2.1 The d4PDF data

The d4PDF is a database that consists of global warming simulations conducted by the climate model MRI- AGCM3.2 from the Meteorological Research Institute under the Japan Meteorological Agency.(Mizuta et al., 2016) The MRI-AGCM3.2 is an atmospheric general circulation model with the capacity of globally simulating the climate for a grid as small as 20km. (Mizuta et al., 2012) The global d4PDF data uses a grid spacing of 60km however, using downscaling for the 20km grid size in the database's regional data for Japan. The global database experiments can be divided into three parts;

- historical climate simulation: 1951-2010
- non-warming simulation: 1951-2010
- +4K future climate simulation: 2051-2110

In this study the non-warming simulations are not analyzed or included in any way. For the future climate simulations, the d4PDF uses the GHG concentration according to the RCP8.5 scenario in 2090 along with the sea-surface temperature (SST) of a 4°C warmer climate at the end of the century (compared to pre-industrial temperatures), which corresponds to the warming in RCP8.5 at the end of the 21st century. The SST temperature is the lower boundary condition for the model and the global mean GHG concentrations, ozone and aerosol distributions the external forcing. The historical and future climate simulations consist of 100 and 90 members respectively where the initial conditions and SST are perturbed for each simulation. Furthermore, the 90 members of the future simulations are based upon the SST warming patterns from 6 different CMIP5 AOGCMs (Table 2.1), resulting in 15 members per model. The long-term trend in the SST temperature is removed for the simulation as to keep the warming constant during the 60-year period. This is different from other experiments in climate modelling where global warming gradually changes during the simulation. This kind of simulation instead provides a larger sampling size for a constant level of warming. (Mizuta et al., 2016)

2.2 The SMHI data

The observation-based result from the SMHI are based on the climate database PTHBV. In this database the data from the observation stations has been interpolated onto a 4km grid using the method called optimal interpolation.

The regional climate data has been downscaled using the regional climate model RCA4 for 9 different global climate models. Since the models have different properties the individual results can deviate from each other. By instead using several climate models the result is more reliable and the deviation between them can be calculated. The climate research unit Rossby Center performed the modeling based on the 9 global models from different institutes, seen in Table 2.1. One simulation was performed each for RCP4.5 and RCP8.5, totaling 18 simulations and the grid size is 50km. In some cases, when the data is used for hydrological studies, the data has been further scaled using the DBS-method (Distribution Based Scaling) to the same grid as the observation data. (Eklund et al., 2015)

2.3 Differences in time period

When studying changes in the climate the future averages are compared to a reference period. The SMHI uses the widespread standard normal period of 1961-1990 most often. While the future climate is often represented by 2069-2098. In the d4PDF there is data from 1951-2010 for the present climate and thus when performing the analysis, the data for the standard normal period has been separated. The d4PDF future simulations encompass the years 2051-2110. Here there is an important difference; since the d4PDF simulations are “constant” (the GHG concentration is not changing and the SST has had its trend removed) all the future data can be used together. This is especially useful hen studying extreme weather events since it gives a larger sampling size. However, the future climate comparisons are not a complete match with regards to the simulation conditions and time period.

2.4 Analysis method

Daily values for temperature and precipitation (daily average for temperature, daily sum for precipitation) in the d4PDF data was imported into MATLAB. Thereafter it was sorted into multi-dimensional matrices with longitude and latitude, and different time divisions (year, member, model, seasons). Then the data could be handled to calculate different means but also be searched for extreme weather events.

When visualizing the data, a projection was applied as to give the proper dimensions. Being located so far north and being an elongated country the distance between two longitudes in the north is about half that which it is in the south. This actually also gives rise to the fact that the grid size is not evenly 60km. The model results are presented in a grid with even latitudinal and longitudinal spacing which result in the longitudinal spacing being roughly 40km in the south and 20 km in the north. The SMHI regional climate models does not have the same situation as it is dealt with during the downscaling. Additionally, the matrices can have a mask applied, separating a certain region from the data which was used to only visualize and calculate for the grid point inside the borders. However, as can be seen in the results, it does not cut off exactly on the border due to the interpolation when plotting.

Table 2.1: The global climate models that are used in the SMHI ensemble and for the d4PDF future SST.

Institute	**SMHI**	**d4PDF**
CCCma, Canada	CanESM2	
CNRM CERFACS, France	CNRM-CM5	
GFDL, USA	GFDL-ESM2M	GFDL CM3
ICHEC, EU	EC-EARTH	
IPSL, France	IPSL-CM5A-MR	
MIROC, Japan	MIROC5	MIROC5
MOHC, UK	HadGEM2-ES	HadGEM2-AO
MPI, Germany	MPI-EMS-LR	MPI-ESM-MR
MRI, Japan		MRI-CGCM3
NCAR, USA		CCSM4
NCC, Norway	NorESM11-M	

2.4.1 Extreme events and return periods

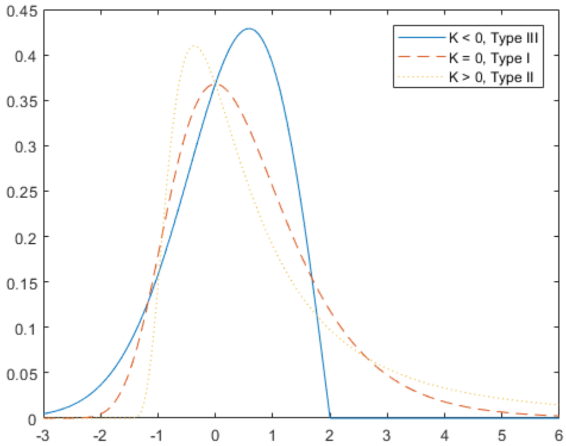

Figure 2.1: The three types of distributions combined in the general extreme value distribution. (MATLAB, n.d.)

Extreme events, as described in section 1.3, can be understood by considering probability distributions. For example, the temperature in one location over a year could be distributed as a normal distribution, but not necessarily so due to the changing conditions (for example seasons) over the year. Irrespective of this, extreme weather behaves differently. Since the extreme events are the maximum or minimum during a time period only that one value would be collected from each year, for example the maximum daily temperature - the warmest day of the year. If these extreme values are collected over many years, these can be represented by a distribution themselves. Although for the extreme values the distribution does not follow the normal distribution, but instead often a so called extreme value distribution.

In this study, the General Extreme Value (GEV) distribution was used to describe extreme events. It is a combination of three simpler distributions, allowing a continuous range of possible shapes and thus allowing the data to influence the distribution to a higher degree. The three distributions are the Gumbel, Fréchet and Weibull distributions and can be seen in Figure 2.1 as type I, II and III respectively. (MATLAB, n.d.)

The return period (RP) is the amount of time that can be expected to pass until a certain value is exceeded again, also called the recurrence interval or repeat interval, and indicates the likelihood of an event based on preexisting data. The return period **T** for an annual maximum event, can be calculated through the probability of exceedance **Pe** and the GEV cumulative distribution function **Pc** via;

$$Pe(x) = 1 - Pc(x) \qquad T(x) = \frac{1}{Pe(x)}$$

(Holthuijsen, 2007) Moreover, the RP can be calculated from the raw data with;

$$RP = \frac{n+1}{m}$$

n, number of years on record
m, number of recorded occurrences of the event

thus, by sorting the data by severity it can be displayed separately as in the results, where also the raw data points are plotted for the present data. This is to control that the two does not deviate to much from each other as that would indicate a bad match of the GEV distribution. For rare events the uncertainty of the GEV distribution grows larger and thus the raw data can naturally deviate more.

3 Results and Discussion

The result is here divided into two subsections. The first pertains to changes related to temperature such as changes in seasonal temperature averages, yearly maximum temperature (daily average) and the length of heat waves. The second part deals with changes in precipitation and includes yearly maximums in short and long periods of precipitation, droughts and seasonal averages. Throughout the results comparisons will be made, when available, to corresponding information from the SMHI ensemble. This results in there being some differences in map color between the SMHI and d4PDF figures unfortunately.

In appendix A, the spread in the results from the 9 SMHI models and the 6 SST datasets in the d4PDF can be seen and compared. Overall the SMHI models have a larger spread in the results, probably due to the actual climate modes being different and not just the SSTs.

3.1 Temperature

Comparing the average temperature in Sweden according to the d4PDF with measurements from the SMHI reveals that the temperature differs very little in the majority of the country as seen in Figure 3.1.

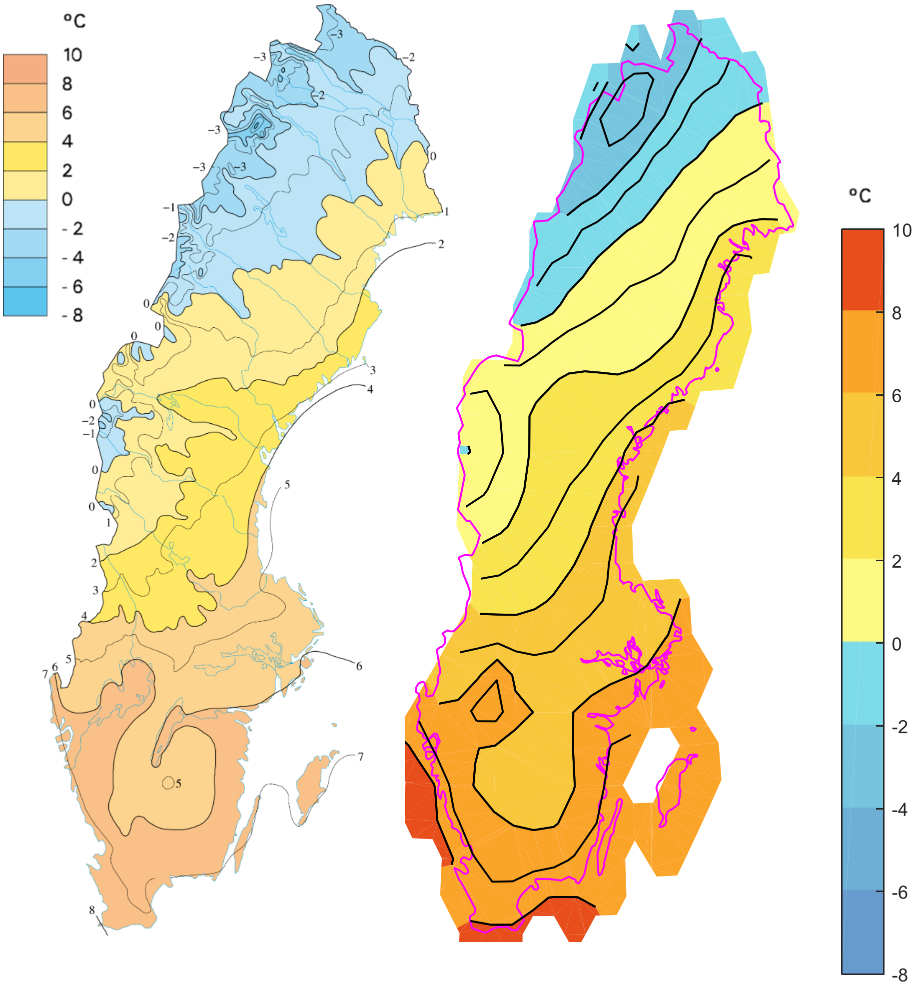

Figure 3.1: The average temperature in Sweden during 1961-1990 according to measurement data from the SMHI to the left and according to the d4PDF to the right.

3.1.1 Annual average temperature change

Maps over the change in yearly average temperature in Sweden from 1961-1990 to the future climate is presented in Figure 3.2. As seen in the figure, temperature increases in the whole country and it increases the most in the northern parts. The same pattern is seen in the previous work conducted by the SMHI. The temperature increase is slightly (~0.5°C) higher in the SMHI ensemble.

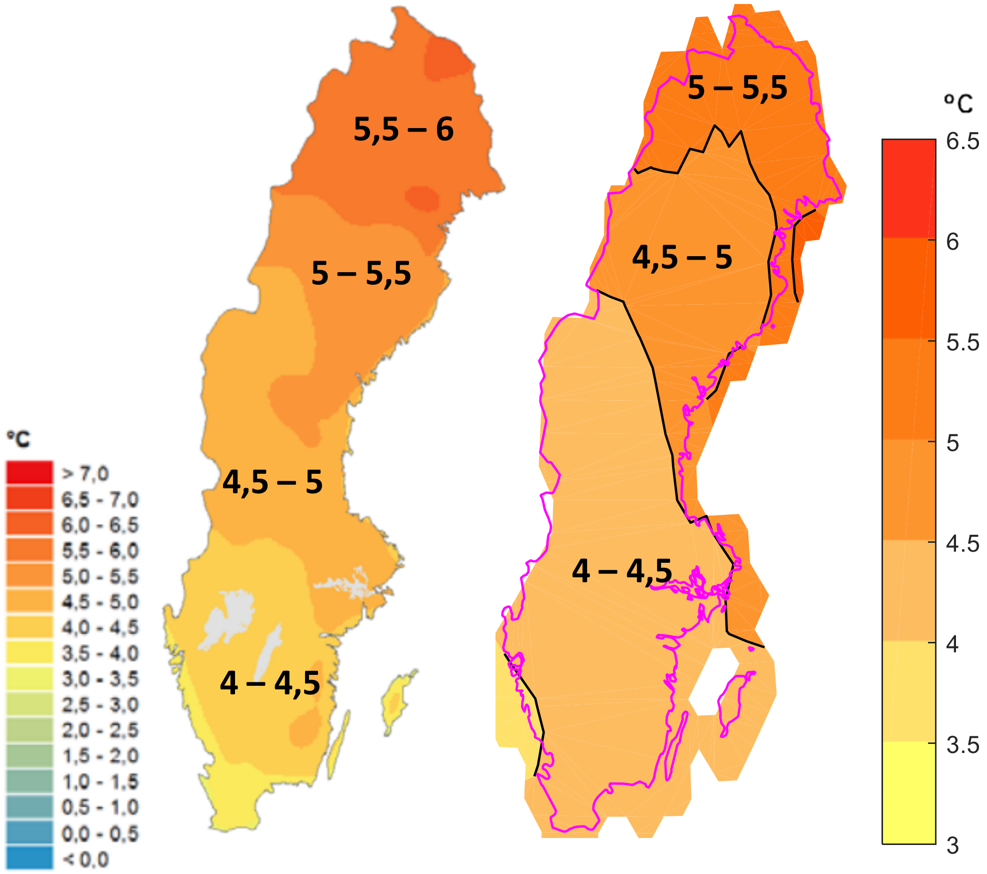

Figure 3.2: Annual mean temperature change (deg. C). Left: The SMHI RCP8.5 increase from 1961-1990 to 2069-2098 (Eklund et al., 2015)*. Right: d4PDF increase from 1961-1990 to future climate.*

Average temperature change in winter

The calculated average change in winter (December, January and February) is presented in Figure 3.3. In winter the temperature increases more than the annual average and the highest increase occurs in the north. When compared to the SMHI ensemble the pattern is similar, but the increase is lower in the d4PDF data.

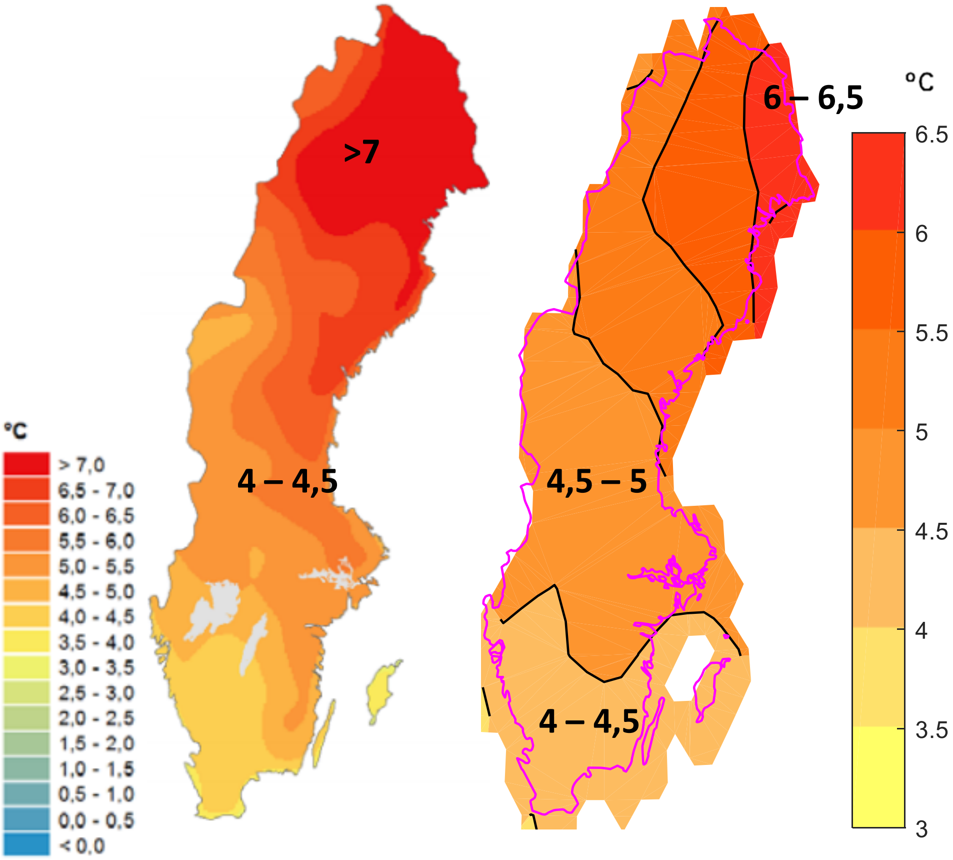

Figure 3.3: Winter mean temperature change (deg. C). Left: The SMHI RCP8.5 increase from 1961-1990 to 2069-2098 (Eklund et al., 2015). *Right: d4PDF increase from 1961-1990 to future climate.*

Average temperature change in spring

The calculated average change in spring (March, April and May) is presented in Figure 3.4. For the d4PDF data; in spring the temperature increases slightly less than the annual average. The temperature increases the most in north Sweden and the warming pattern differs somewhat to the SMHI models.

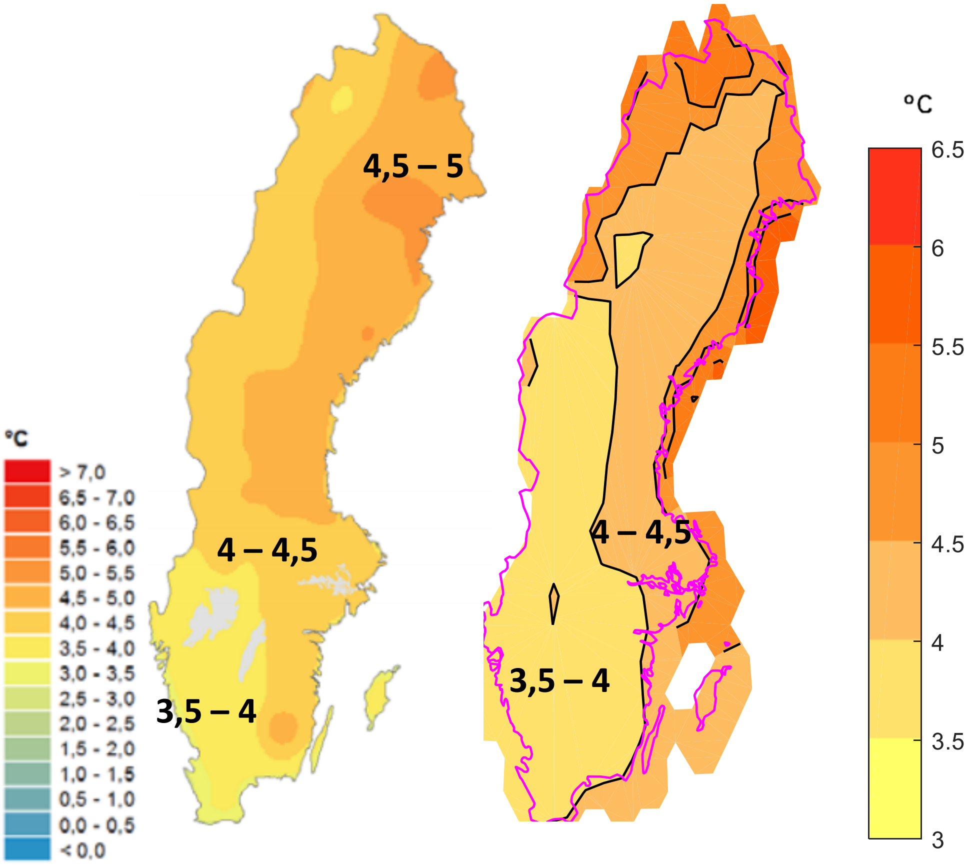

Figure 3.4: Spring mean temperature change (deg. C). Left: The SMHI RCP8.5 increase from 1961-1990 to 2069-2098 (Eklund et al., 2015)*. Right: d4PDF increase from 1961-1990 to future climate.*

Average temperature change in summer

The calculated average change in summer (June, July and August) is presented in Figure 3.5. In summer the temperature increases less than the annual average. When comparing the warming pattern to the SMHI ensemble, the warming is generally lower in the d4PDF data, especially in the north-west where there is a higher increase.

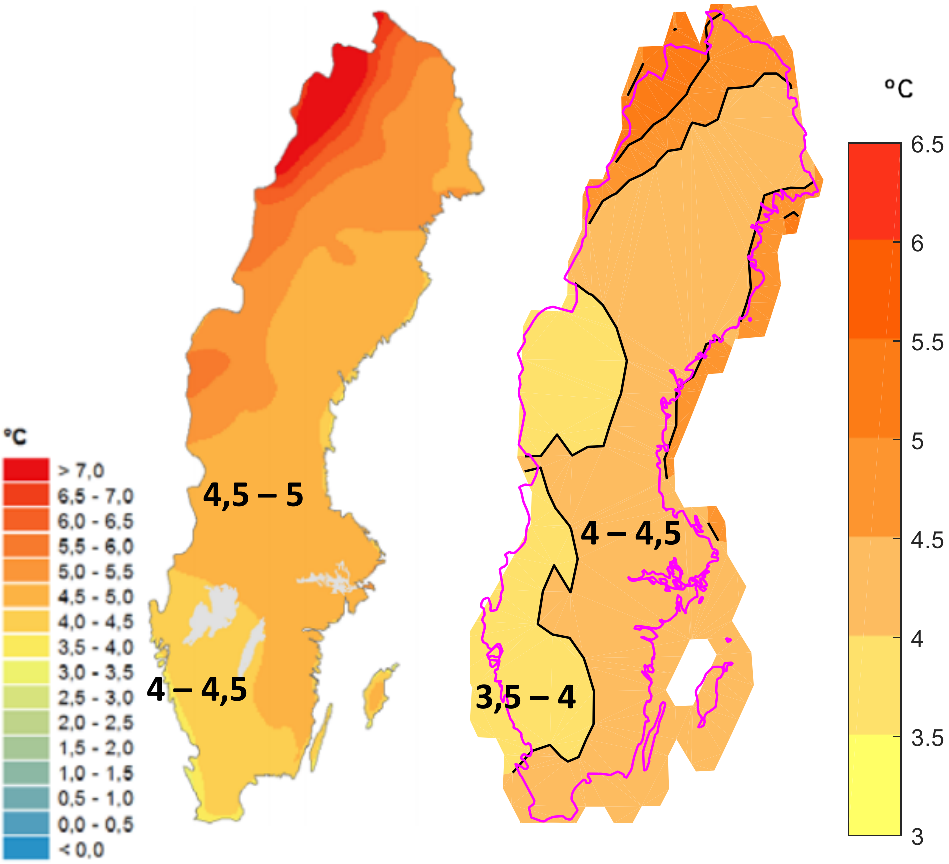

Figure 3.5: Summer mean temperature change(deg. C). Left: The SMHI RCP8.5 increase from 1961-1990 to 2069-2098 (Eklund et al., 2015). *Right: d4PDF increase from 1961-1990 to future climate.*

Average temperature change in autumn

The calculated average change in autumn (September, October and November) is presented in Figure 3.6. In autumn the temperature increases about the same as the annual average. When comparing the warming pattern to the SMHI ensemble, they are mostly similar except a slightly higher increase in the d4PDF data for the southern half of Sweden.

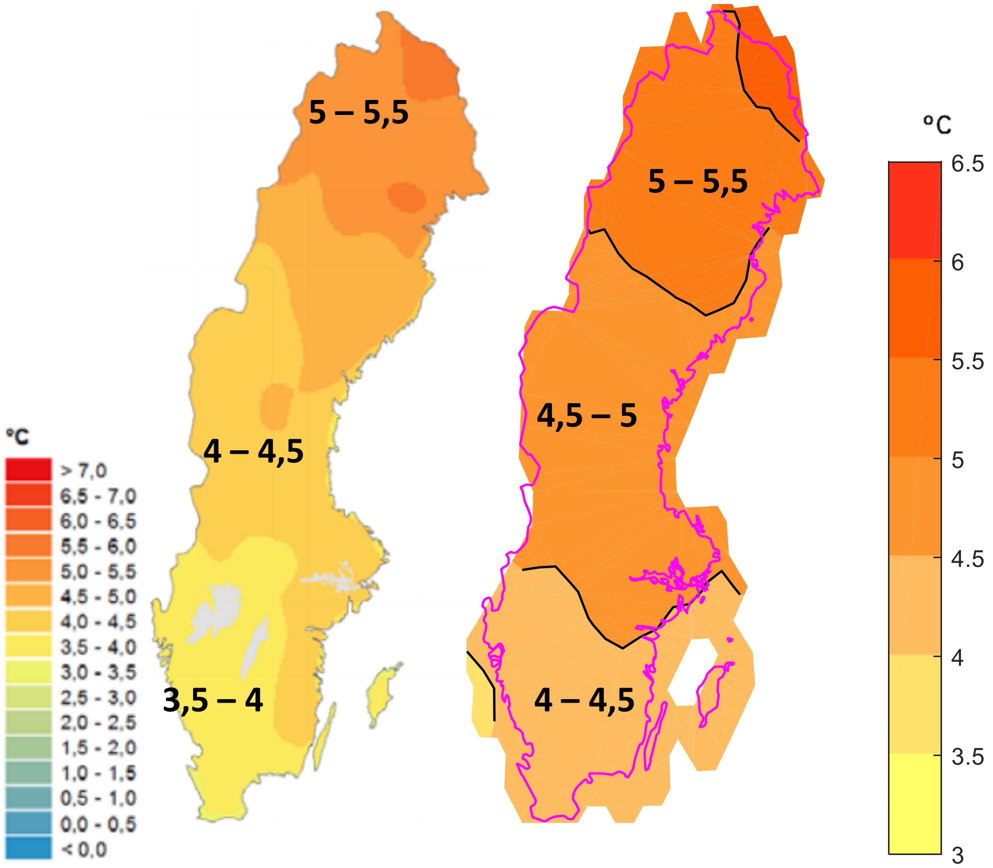

Figure 3.6: Autumn mean temperature change(deg. C). Left: The SMHI RCP8.5 increase from 1961-1990 to 2069-2098 (Eklund et al., 2015)*. Right: d4PDF increase from 1961-1990 to future climate.*

3.1.2 Maximum daily temperature

The median maximum daily temperature, i.e. the warmest day of the year, increases by about 4°C in the whole country from 1961-1990 to the future climate according to the d4PDF data as seen in Figure 3.7. The SMHI ensemble has shown the same increase in most of Sweden from 1971-2000 to 2071-2100, except in the northern most parts. (SMHI, n.d.)

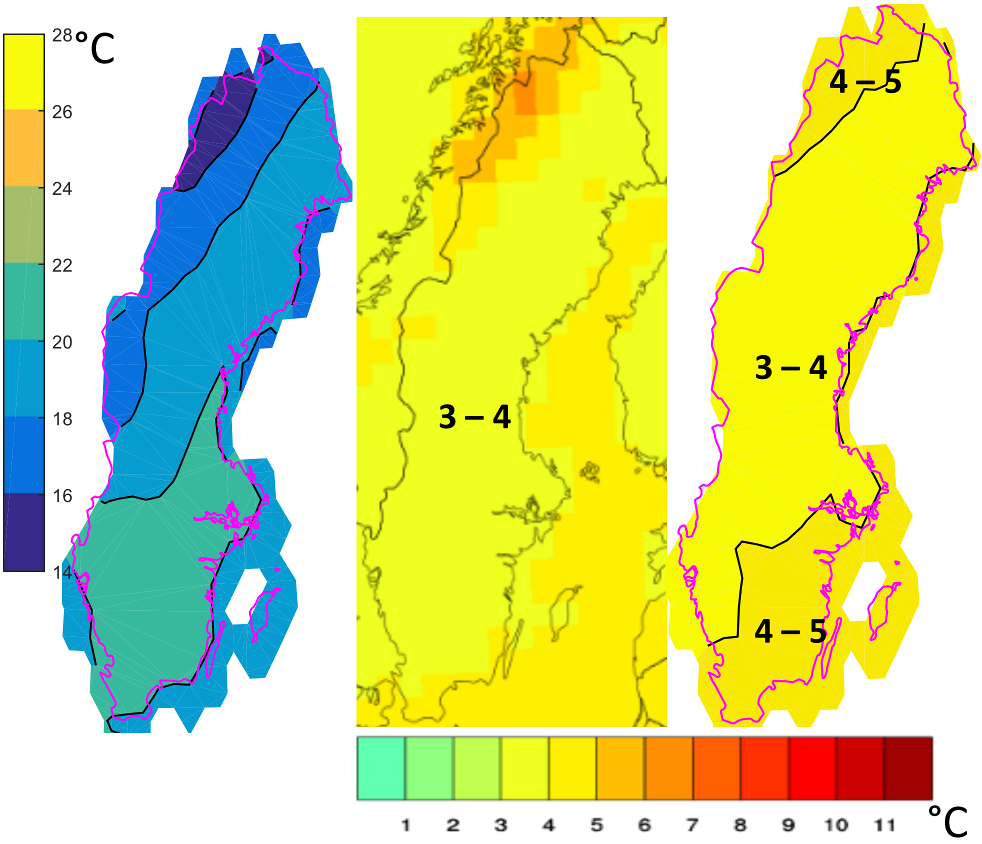

Figure 3.7: The median maximum daily temperature in current climate from the d4PDF (left). The median maximum daily temperature change from the SMHI (middle) and d4PDF (right).

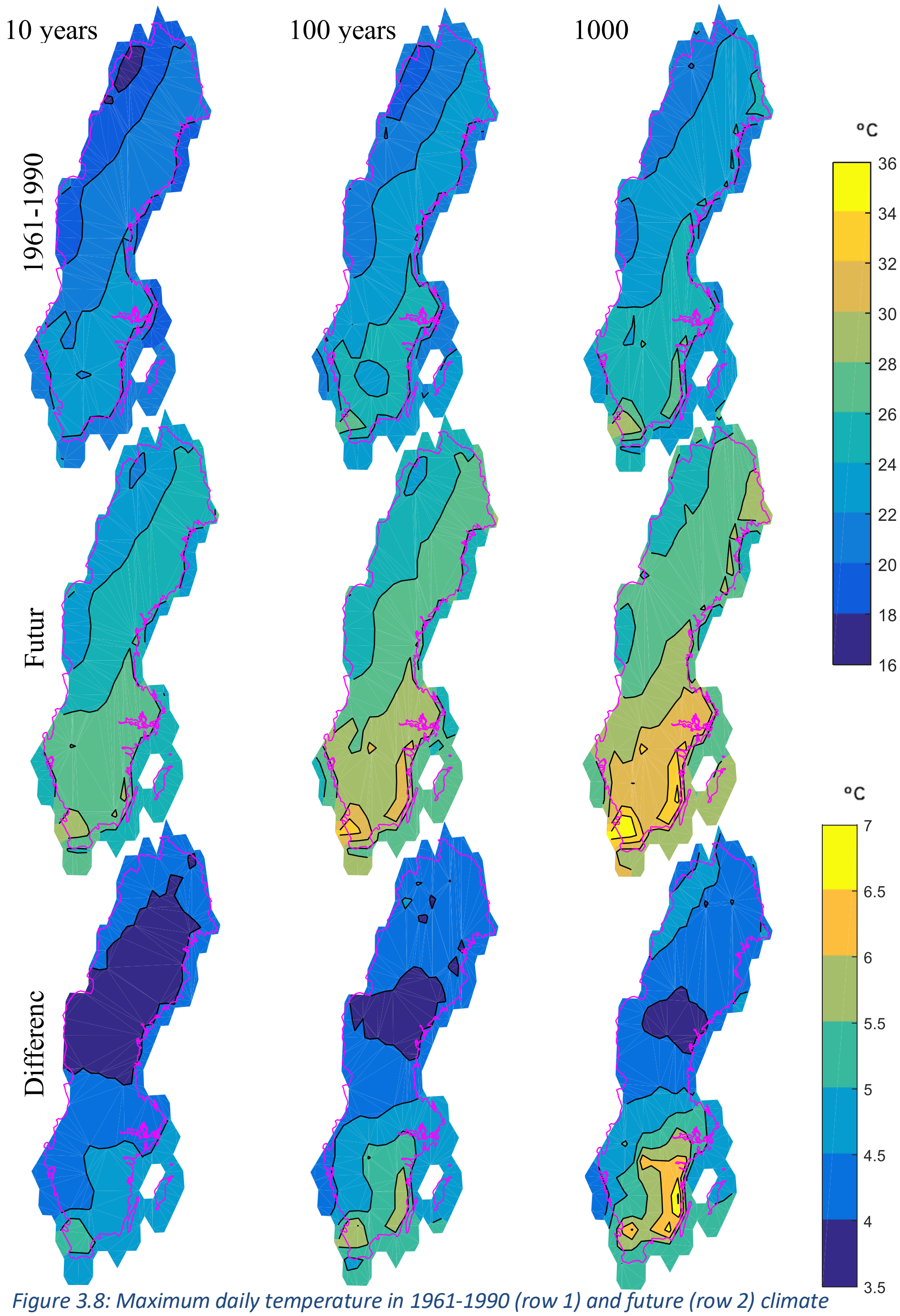

Figure 3.8: Maximum daily temperature in 1961-1990 (row 1) and future (row 2) climate and the difference between them (row 3) for return periods of 10, 100 and 1000 years (column 1, 2 and 3 respectively). Made from the GEV distribution for each grid point. (°C)

When analyzing the warmest day of the year it shows that most often it increases to the same degree as the average temperature increase in Sweden during summer. The exception being for very rare events with return period of more than 100 years in south/south-east Sweden where the warmest day is more than 5 degrees warmer as seen in Figure 3.8.

If the maximum daily temperature is instead plotted for all of Sweden, i.e. the warmest day for each year regardless of the location, the return period plot in Figure 3.9 can be made. The return period plot in Figure 3.9 shows that the maximum daily temperature for all of Sweden increases 4-6°C, the most for long return periods. The raw data points align well with the GEV-calculated line which supports the choice of distribution.

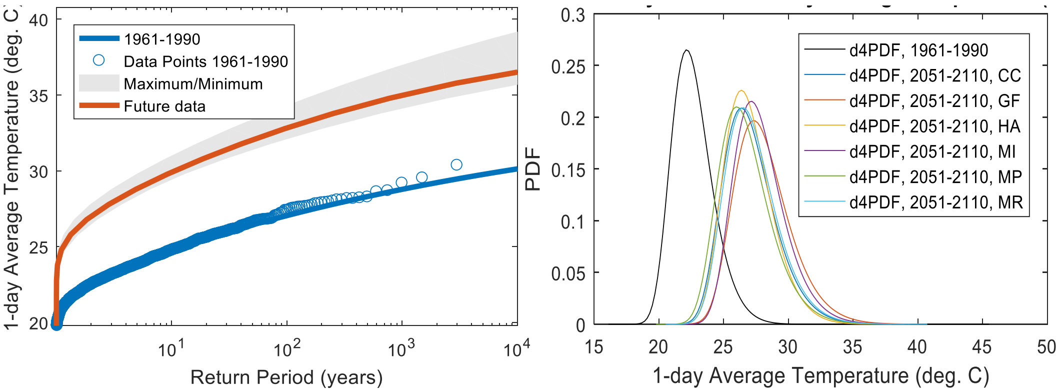

Figure 3.9: Right: The return period plot for 1961-1990 (blue) and the d4PDF future (red) data of the maximum daily temperature in Sweden. The future data plot shows the mean of all 6 models as the red line and the maximum/minimum model as the shaded area. The present data plot shows the individual data points as circles and the calculated GEV-data as the blue line.
Left: The probability density function of the present climate data and the 6 future climate models.

3.1.3 Heat wave length

The length of heat waves in Sweden, i.e. the highest number of consecutive days with a daily mean temperature above 20°C, increases in the whole country as can be seen in Figure 3.10. The comparison between the SMHI and the d4PDF is less clear as the SMHI data has been further scaled for hydrological studies.

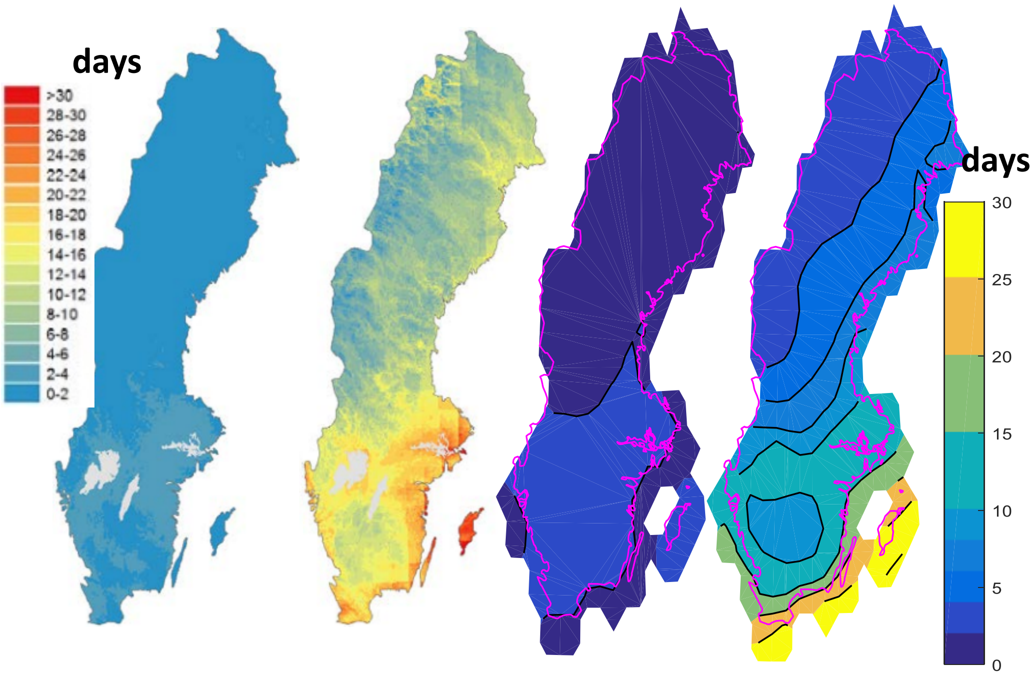

Figure 3.10: The yearly maximum heat wave length (days) in present and future climate. Left: SMHI ensemble results for 1961-1990 (left) and 2069-2098 (right). (Eklund et al., 2015) *Right: d4PDF results for 1961-1990 and the simulated future data.*

3.2 Precipitation

The current yearly average precipitation in Sweden according to measurements and the d4PDF is shown in Figure 3.11. Generally, the d4PDF shows a higher amount of precipitation in most parts but the regional precipitation pattern is similar.

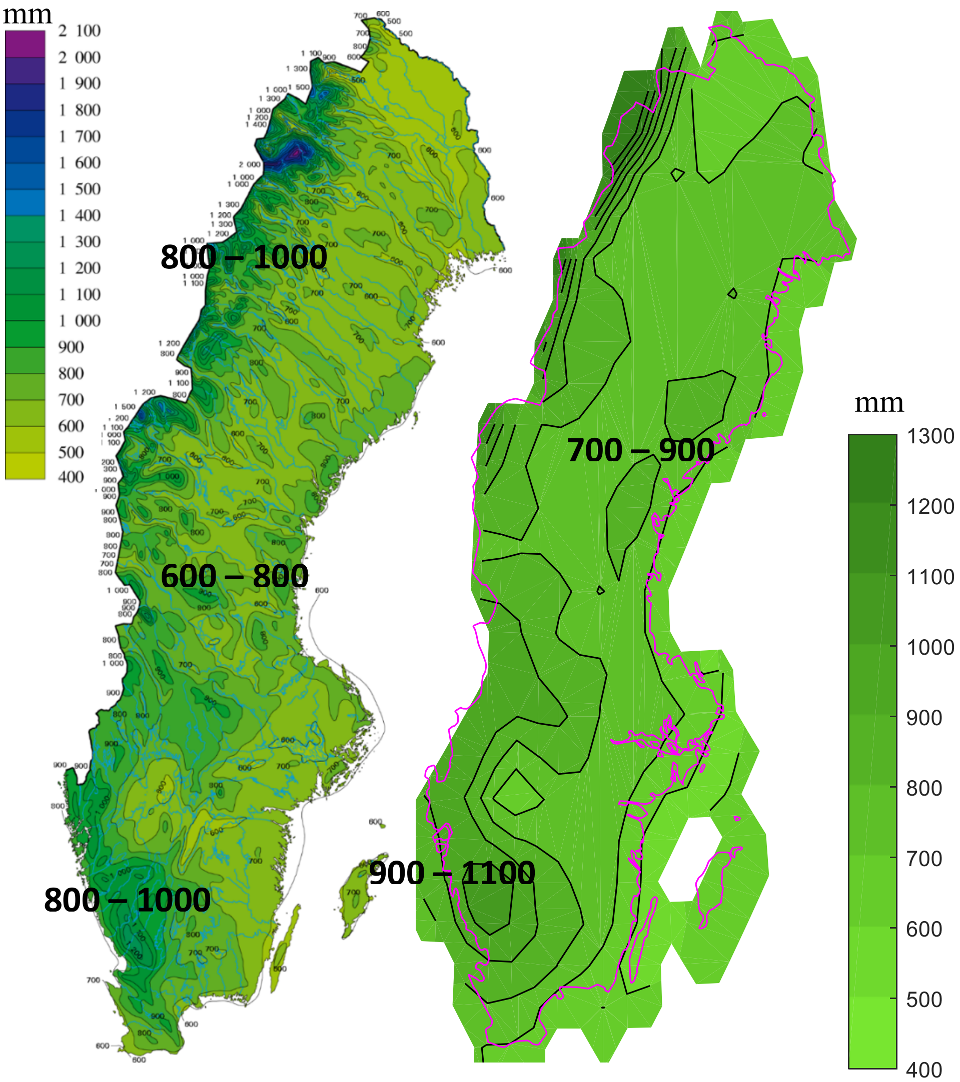

Figure 3.11: The average precipitation (mm) in Sweden during 1961-1990 according to measurement data from the SMHI (SMHI, 2009b) to the left and according to the d4PDF to the right.

3.2.1 Annual precipitation

The annual average precipitation (Figure 3.12) increases in the whole country according to both SMHI and the d4PDF data. The highest increase occurs in the north and the lowest in the south, similar to the temperature change. On average the precipitation increase is ~20%.

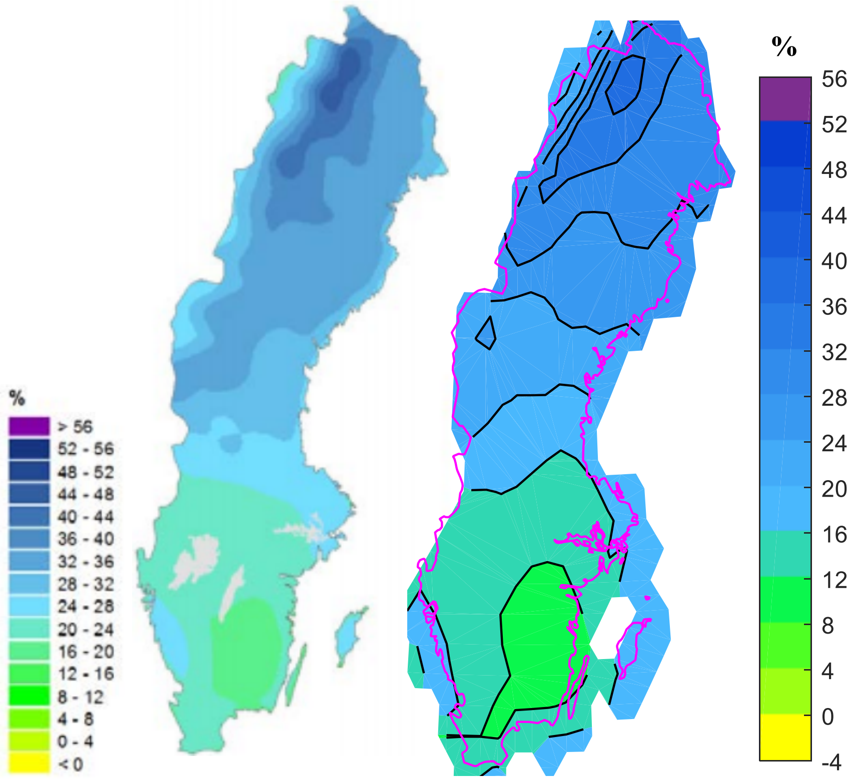

Figure 3.12: Annual mean precipitation change(%). Left: The SMHI RCP8.5 increase from 1961-1990 to 2069-2098 (Eklund et al., 2015). *Right: d4PDF increase from 1961-1990 to future climate.*

Precipitation in winter

During the winter months the precipitation increases the most. Also here there is an increasing gradient from the south to the north as seen in Figure 3.13. The increase pattern in the d4PDF is quite similar to the SMHI.

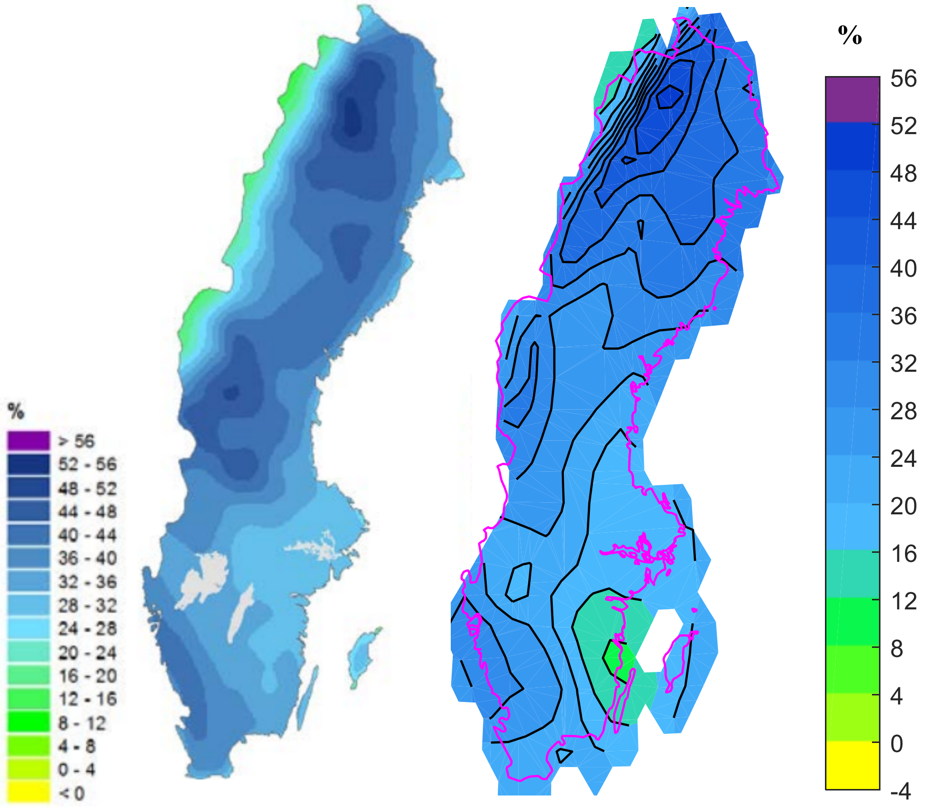

Figure 3.13: Winter mean precipitation change(%). Left: The SMHI RCP8.5 increase from 1961-1990 to 2069-2098 (Eklund et al., 2015)*. Right: d4PDF increase from 1961-1990 to future climate.*

Precipitation in spring

In spring the increase is second highest, and the change pattern is similar between the SMHI and d4PDF, Figure 3.14. Also here the increase is highest in the north.

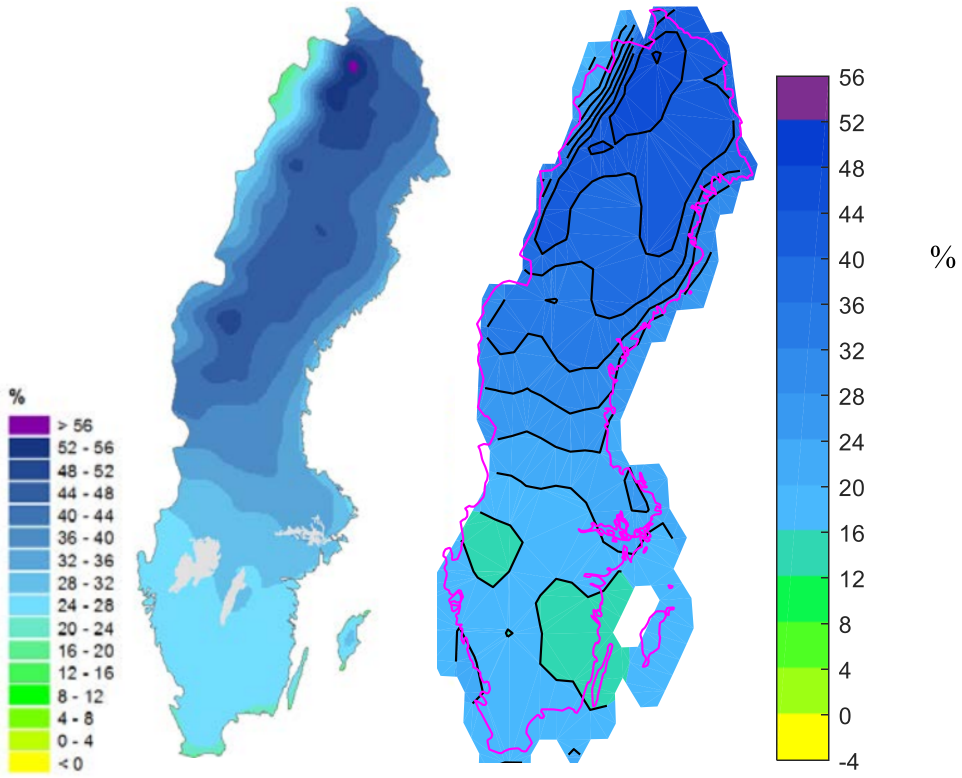

Figure 3.14: Spring mean precipitation change(%). Left: The SMHI RCP8.5 increase from 1961-1990 to 2069-2098 (Eklund et al., 2015). *Right: d4PDF increase from 1961-1990 to future climate.*

Precipitation in summer

In summer there is actually a slight decrease in precipitation for south Sweden according to the d4PDF, Figure 3.15. This decrease is not seen in the SMHI data, but the increase is the lowest.

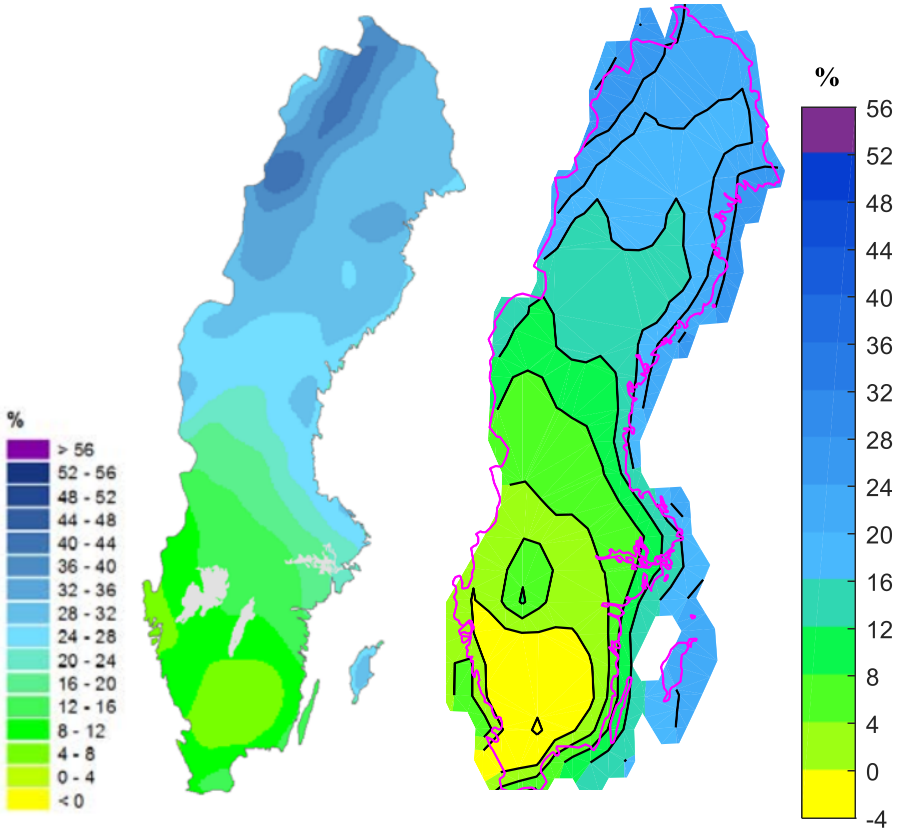

Figure 3.15: Summer mean precipitation change(%). Left: The SMHI RCP8.5 increase from 1961-1990 to 2069-2098 (Eklund et al., 2015). *Right: d4PDF increase from 1961-1990 to future climate.*

Precipitation in autumn

Similar to the other seasons, in autumn the precipitation increases in the same pattern. The highest increase occurs in the northern parts of the country.

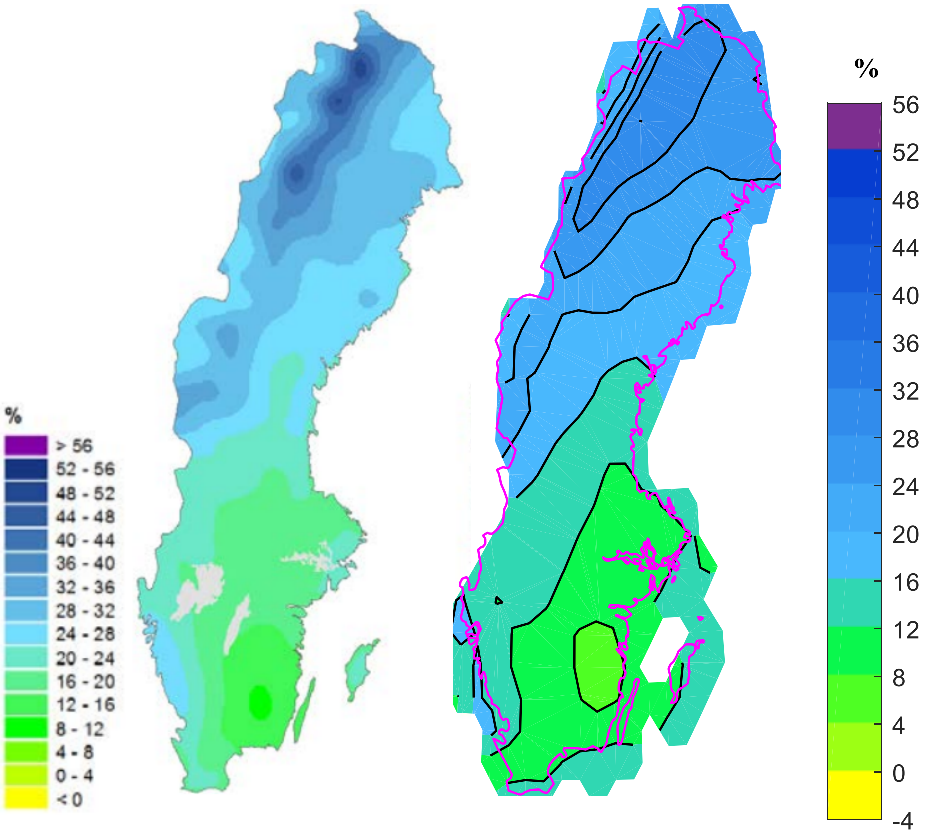

Figure 3.16: Autumn mean precipitation change(%). Left: The SMHI RCP8.5 increase from 1961-1990 to 2069-2098 (Eklund et al., 2015)*. Right: d4PDF increase from 1961-1990 to future climate.*

3.2.2 Maximum daily precipitation

The median maximum daily precipitation, the day of the year with the highest amount of precipitation, increases by approximately 25% quite evenly across the country in both SMHI data and the d4PDF. (Figure 3.17)

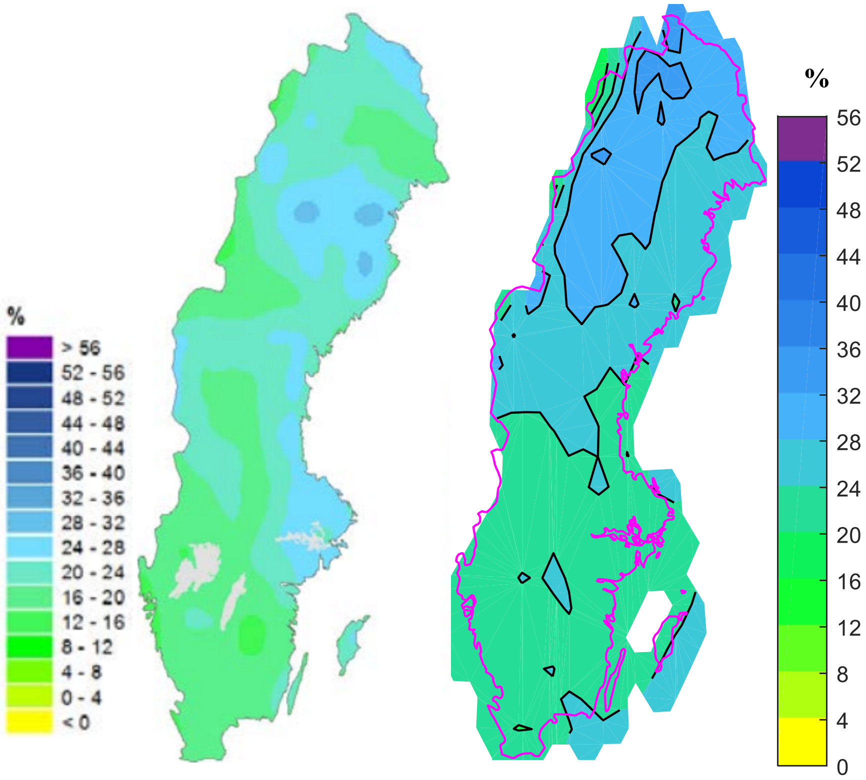

Figure 3.17: The increase in median maximum daily precipitation. Left: SMHI from 1961-1990 to 2069-2098. (Eklund et al., 2015) *Right: d4PDF from 1961-1990 to the future data.*

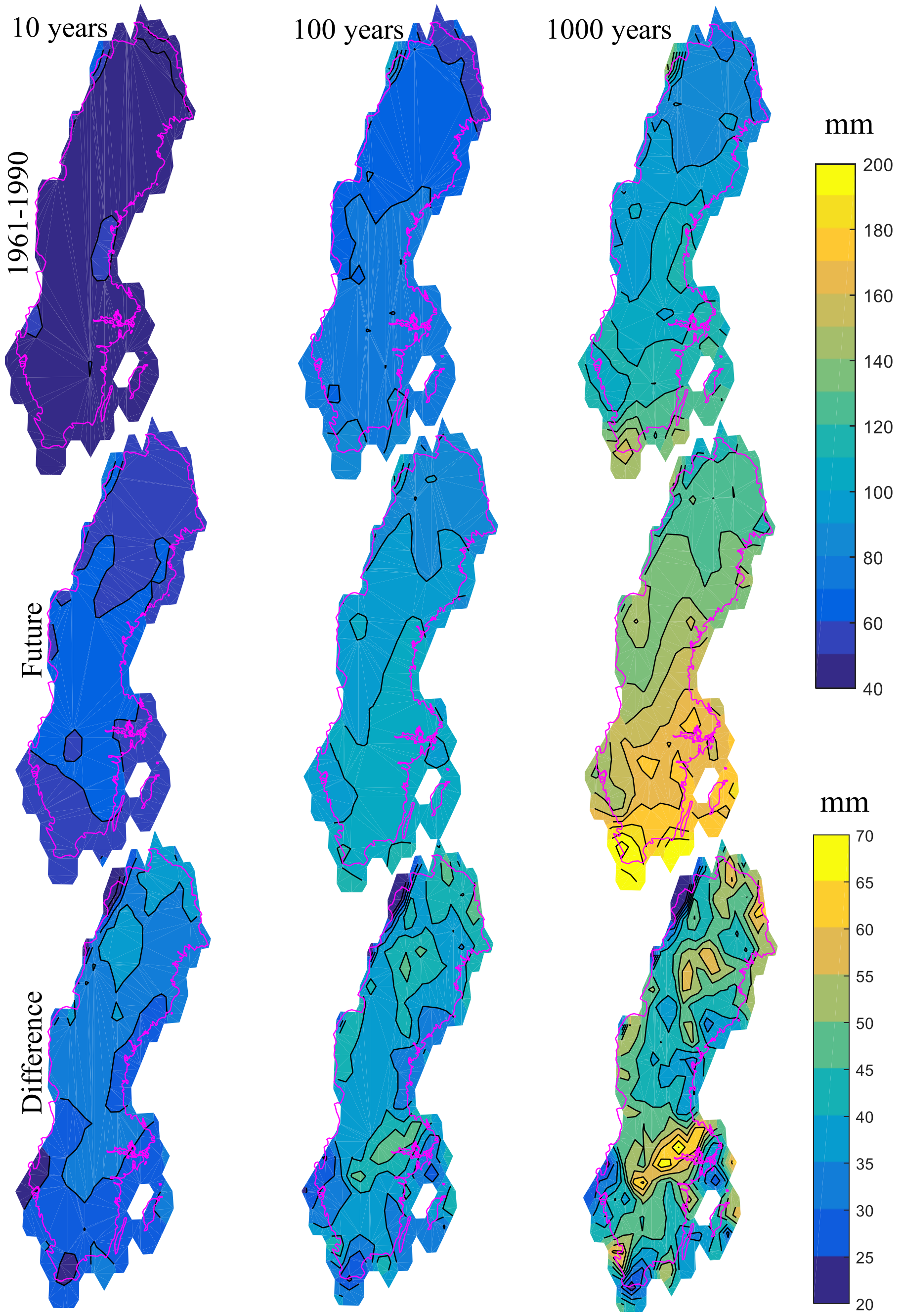

Figure 3.18: Maximum daily precipitation in 1961-1990 (row 1) and future (row 2) (mm) climate and the difference between them (row 3) for return periods of 10, 100 and 1000 years (column 1, 2 and 3 respectively). (%)

When studying the daily maximum precipitation for different return periods as in Figure 3.18 one can clearly see that the precipitation increases significantly more for very rare events. This makes the precipitation climate more unstable as the rare events become even more extreme compared to the usual precipitation levels. This can also be seen if the maximum daily precipitation for the whole country for each year is plotted as in Figure 3.19. The longer return periods increase more, >50%, while the shorter not as much, <35%. In Figure 3.19, the raw data points correspond well to the GEV-derived line for the most part. The highest value deviates quite a bit, but the uncertainty of the plot grows for longer return periods.

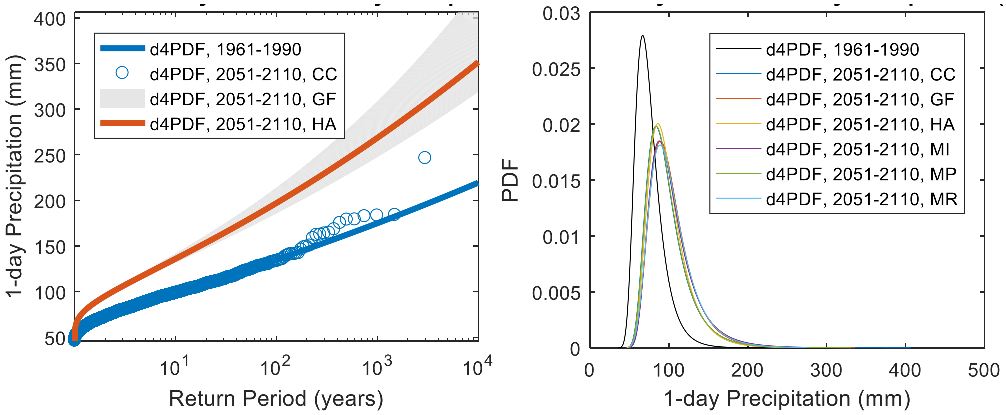

Figure 3.19: Right: The return period plot for 1961-1990 (blue) and the d4PDF future (red) data of the maximum daily precipitation in Sweden (mm). The future data plot shows the mean of all 6 models as the red line and the maximum/minimum model as the shaded area. The present data plot shows the individual data points as circles and the calculated GEV-data as the blue line.
Left: The probability density function of the present climate data and the 6 future climate models.

3.2.3 Maximum 7-day precipitation

The maximum 7-day precipitation also increases, as seen in Figure 3.20, but it does so quite evenly for all return periods. When comparing the maximum 7-day precipitation return period plot to the 1-day return period in Figure 3.19 it can clearly be observed that the longer duration event increase much less than the shorter duration events.

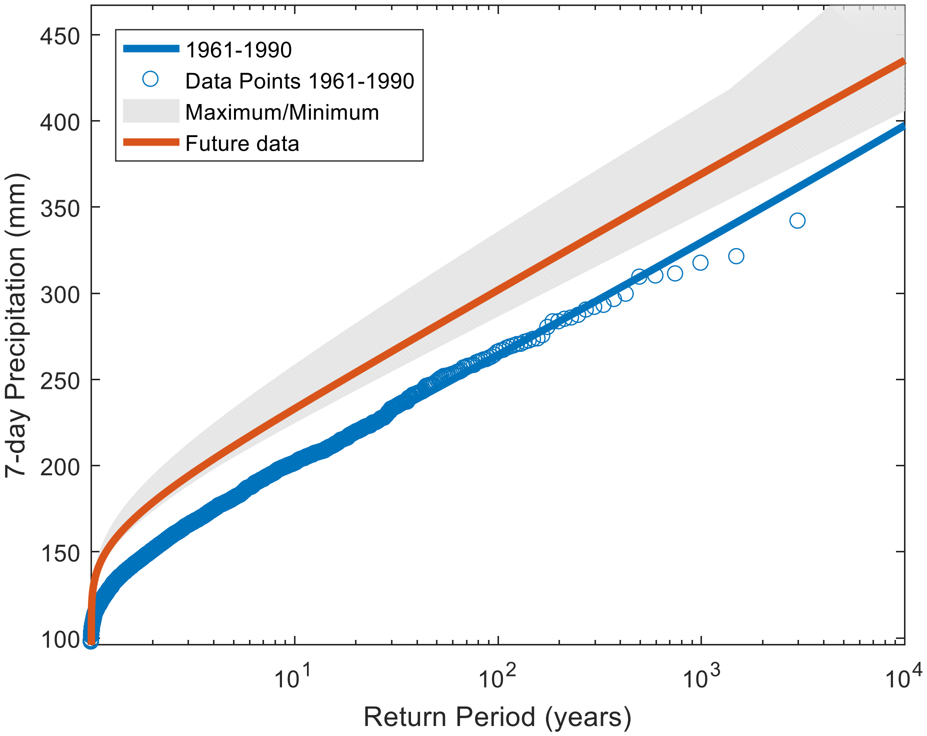

Figure 3.20: The return period plot for 1961-1990 (blue) and the d4PDF future (red) data of the maximum 7-day precipitation in Sweden (mm). The future data plot shows the mean of all 6 models as the red line and the maximum/minimum model as the shaded area. The present data plot shows the individual data points as circles and the calculated GEV-data as the blue line.

3.2.4 Longest drought duration

The longest drought duration for the whole country in year, defined as the number of consecutive days with precipitation <1mm, does not change especially much and it is hard to say if the change is significant (see Figure 3.21). However, the definition of a drought here is somewhat lacking. It should include the change in evapotranspiration from the increasing temperature as well. Therefore, it is difficult to draw any further conclusions since it is oppositely affected by the increasing precipitation and the increasing temperature.

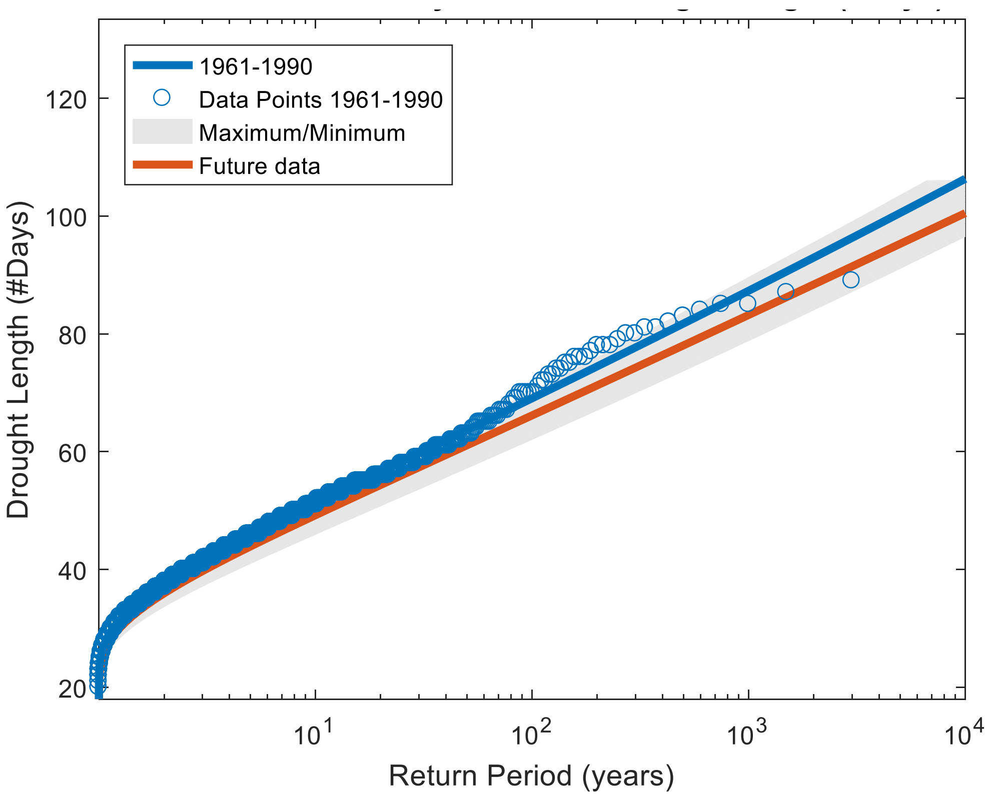

Figure 3.21: The return period plot for 1961-1990 (blue) and the d4PDF future (red) data of the longest drought duration in Sweden (number of days). The future data plot shows the mean of all 6 models as the red line and the maximum/minimum model as the shaded area. The present data plot shows the individual data points as circles and the calculated GEV-data as the blue line.

4 Conclusions

The MRI-AGCM model used by the d4PDF gave a similar temperature and precipitation climate as measurements and future simulations from the SMHI. The temperature in Sweden is bound to increase more than the global average and especially so in the northern parts during winter and autumn according to the d4PDF. In the SMHI ensemble the seasonal temperature increases more during summer than autumn. This is one of the few deviations between the ensembles. The reason can only be internal differences in the models used or possible due to a time period mismatch. Because of the temperature increase the heat wave length increases as well, which could result in hazardous temperatures for more sensitive population groups. Keep in mind that the temperature plotted is the daily average temperature and that the temperature during daytime is likely a couple of degrees higher. This could also result in the increased need of some sort of air conditioning in both private homes businesses as it is rarely used currently during temperate summers. Also, in the south the highest temperatures of the year increase more for rare events, for long return periods, which indicates a more unpredictable temperature climate. Higher temperatures increase the need of proper irrigation in agriculture, this could possibly cause problems in the south-east where the precipitation also decreases during summer months. The south-east is also where the most intensive agriculture is because of the relatively flat landscape with rich soil.

The yearly precipitation increases on average by roughly 20% in both the SMHI and d4PDF data and the maximum daily precipitation by about the same amount, ~25%. However, intense events with long return periods increase more than 50%, while more common intense events increase less <35%. Longer duration events do not increase as much and the change is about the same for short and long return periods, ~15%. The highest increase in precipitation occurs in the north during winter and spring in both the SMHI and d4PDF and in summer the south parts there is almost no change in both cases. There is a slight decrease in the d4PDF and a slight increase in the SMHI data.

The changes will interact with each other, causing changes in the growth season and thus the conditions for Swedish agriculture and industry. The important forestry industry has previously been severely affected mostly by rare storms and forest fires. In the future, climate change could possibly introduce new possible crop choices but also new pests. The risk of forest fires is complicated as it would be lowered by the increase in precipitation but raised by higher temperatures and longer heat waves. North Sweden contains most of the main electricity production facilities, hydropower dams. The changes could be important, considering the precipitation and temperature effect on water retention by snow cover and the spring flood. The hydropower dams were mostly constructed in the mid-20th century and the risk analysis for the dimensioning of the dams possibly should be reviewed. Because the long lifespan of the construction it must be properly dimensioned for future increased risk of high flows that could pose a threat to the integrity of the dam.

The d4PDF database is an excellent tool for analyzing changes in extreme weather. Not only is there a large amount of data in present and future climate, there is also data for a non-warming scenario. The purpose is mainly for attribution studies where the likelihood of occurrence of an event in the present climate can be compared to the likelihood in a climate without anthropogenic climate change. The database is designed for extreme weather studies also through the future climate’s trend cancelling. The trend is removed in the SST change and the GHG concentration is kept constant. This gives a large amount of extreme weather data for a future climate without the need to consider the climate change during each simulation. This however makes the future climate comparison less ideal since the time period cannot be an exact match.

5 References

Eklund, A., Mårtensson, J. A., Bergström, S., Björck, E., Dahné, J., Lindström, L., … Sjökvist, E. (2015). Sveriges framtida klimat: Underlag till Dricksvattenutredningen. *KLIMATOLOGI*, *14*. Retrieved from http://www.smhi.se/polopoly_fs/1.89529!/Menu/general/extGroup/attachmentColHold/mainCol1/file/klimatologi_14.pdf

Flato, G., Marotzke, J., Abiodun, B., Braconnot, P., Chou, S. C., Collins, W., … Rummukainen, M. (2013). Evaluation of Climate Models. In *Climate Change 2013: The Physical Science Basis. Contribution of Working Group I to the Fifth Assessment Report of the Intergovernmental Panel on Climate Change* (pp. 741–866). Cambridge: Cambridge University Press. https://doi.org/10.1017/CBO9781107415324

Holthuijsen, L. H. (2007). *Waves in Oceanic and Coastal Waters* (2009th ed.).

IPCC. (2012). *Managing the Risks of Extreme Events and Disasters to Advance Climate Change Adaptation*. (C. B. Field, V. Barros, T. F. Stocker, D. Qin, D. J. Dokken, K. L. Ebi, … P. M. Midgley, Eds.), *A Special Report of Working Groups I and II of the Intergovernmental Panel on Climate Change*. Cambridge University Press, Cambridge, UK, and New York, NY, USA. Retrieved from https://wg1.ipcc.ch/srex/downloads/SREX-All_FINAL.pdf

IPCC. (2014a). Climate Change 2013 - The Physical Science Basis. *Climate Change 2014: Synthesis Report*, *29*(17), 151. https://doi.org/10.1017/CBO9781107415324

IPCC. (2014b). *Climate Change 2014: Synthesis Report*. Geneva, Switzerland: IPCC. Retrieved from http://www.ipcc.ch/pdf/assessment-report/ar5/syr/SYR_AR5_FINAL_full_wcover.pdf

Klimatanpassningsportalen. (2013). Temperatur. Retrieved February 17, 2018, from http://www.klimatanpassning.se/hur-forandras-klimatet/temperatur-information-1.22491

Klimatanpassningsportalen. (2016). Precipitation. Retrieved February 17, 2018, from http://www.klimatanpassning.se/en/climate-change-in-sweden/precipitation-1.97807

Le Treut, H., Somerville, R., Cubasch, U., Ding, Y., Mauritzen, C., Mokssit, A., … Prather, M. (2007). 2007: Historical Overview of Climate Change. In *Climate Change 2007: The Physical Science Basis. Contribution of Working Group I to the Fourth Assessment Report of the Intergovernmental Panel on Climate Change* (Vol. Chapter 1, pp. 93–127). Cambridge University Press. https://doi.org/10.1016/j.soilbio.2010.04.001

MATLAB. (n.d.). Generalized Extreme Value Distribution. Retrieved February 17, 2018, from https://www.mathworks.com/help/stats/generalized-extreme-value-distribution.html?s_tid=gn_loc_drop

Mizuta, R., Murata, A., Ishii, M., Shiogama, H., Hibino, K., Mori, N., … Kimoto, M. (2016). Over 5000 years of ensemble future climate simulations by 60 km global and 20 km regional atmospheric models. *Bulletin of the American Meteorological Society*, BAMS-D-16-0099.1. https://doi.org/10.1175/BAMS-D-16-0099.1

Mizuta, R., Yoshimura, H., Murakami, H., Matsueda, M., Endo, H., Ose, T., … Kitoh, A. (2012). Climate Simulations Using MRI-AGCM3.2 with 20-km Grid. *Journal of the Meteorological Society of Japan*, *90A*, 233–258. https://doi.org/10.2151/jmsj.2012-A12

MSB. (2017). Naturolycksdatabasen. Retrieved February 17, 2018, from https://www.msb.se/sv/Kunskapsbank/Erfarenheter-fran-olyckor--

kriser/Naturolycksdatabasen/

SMHI. (n.d.). Future climate: Climate scenarios. Retrieved January 18, 2018, from https://www.smhi.se/klimat/framtidens-klimat/klimatscenarier?area=swe&var=t&sc=rcp85&seas=ar&dnr=99&sp=en&sx=0&sy=0

SMHI. (2009a). Hur fungerar en klimatmodell? Retrieved December 8, 2017, from https://www.smhi.se/kunskapsbanken/klimat/hur-fungerar-en-klimatmodell-1.470

SMHI. (2009b). Normal uppmätt årsnederbörd, medelvärde 1961-1990 | SMHI. Retrieved February 2, 2018, from http://www.smhi.se/klimatdata/meteorologi/nederbord/normal-uppmatt-arsnederbord-medelvarde-1961-1990-1.4160

Taylor, K. E., Stouffer, R. J., & Meehl, G. A. (2009). A Summary of the CMIP5 Experiment Design. Retrieved from https://pcmdi.llnl.gov/mips/cmip5/docs/Taylor_CMIP5_design.pdf?id=76

Taylor, K. E., Stouffer, R. J., Meehl, G. A., Taylor, K. E., Stouffer, R. J., & Meehl, G. A. (2012). An Overview of CMIP5 and the Experiment Design. *Bulletin of the American Meteorological Society*, *93*(4), 485–498. https://doi.org/10.1175/BAMS-D-11-00094.1

WRCP. (n.d.). WCRP Coupled Model Intercomparison Project (CMIP). Retrieved January 11, 2018, from https://www.wcrp-climate.org/wgcm-cmip

6 Appendix A. Maps of the spread in results

The maps shown in the results are based on the mean or median of the models for both the 9 SMHI models and the 6 future SST datasets in the d4PDF. In this appendix the maximum and minimum value, regardless of model, is shown in order to give an idea of the spread of the results.

Annual and seasonal average temperature

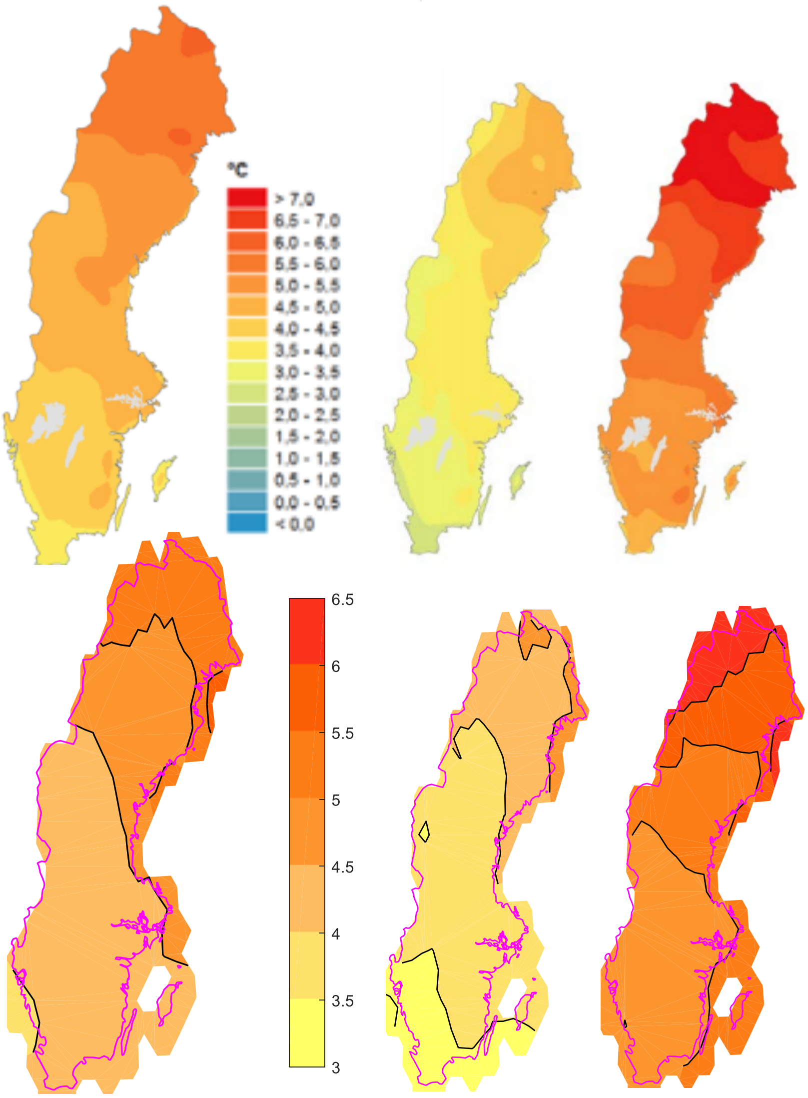

Mean **Min** **Max**

Figure 6.1: The change of the yearly average temperature from 1961-1990 to 2069-2098 for the SMHI data (top) (Eklund et al., 2015) *and from 1961-1990 to the future data in the d4PDF (bottom). The max and min maps show the model result with the maximum and minimum results for each grid point.*

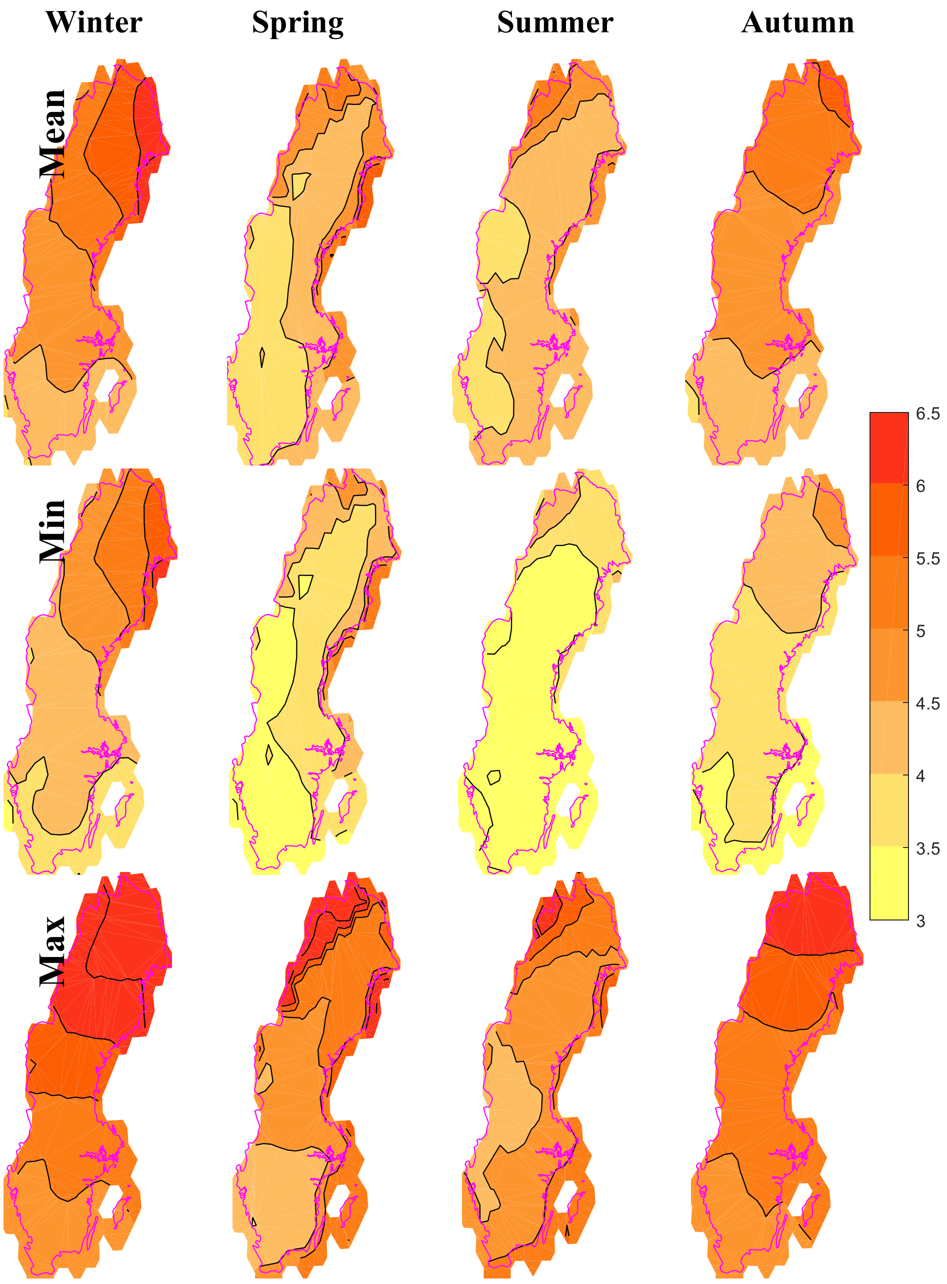

Figure 6.2: The d4PDF seasonal (left to right) temperature increase form 1961-1990 to the future climate. Mean (top), min (middle) and min (bottom). The max and min maps show the model result with the maximum and minimum results for each grid point.

Maximum daily temperature

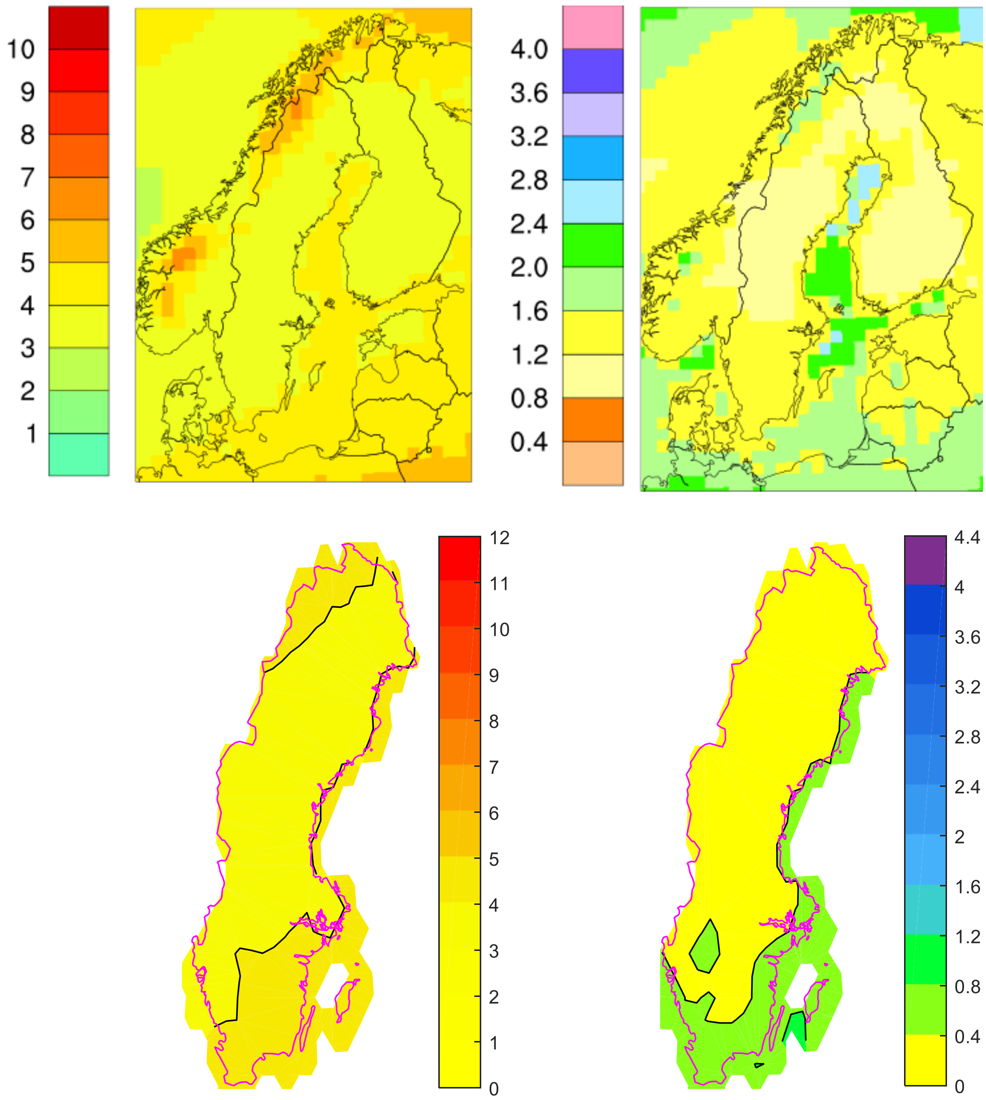

Figure 6.3: The maximum daily temperature increase from 1971-2000 to 2071-2100 for the SMHI and from 1971-2000 to the future climate for the d4PDF data. The median (left) and standard deviation (right) of the models from the SMHI (top) and d4PDF (bottom).

Heat wave length

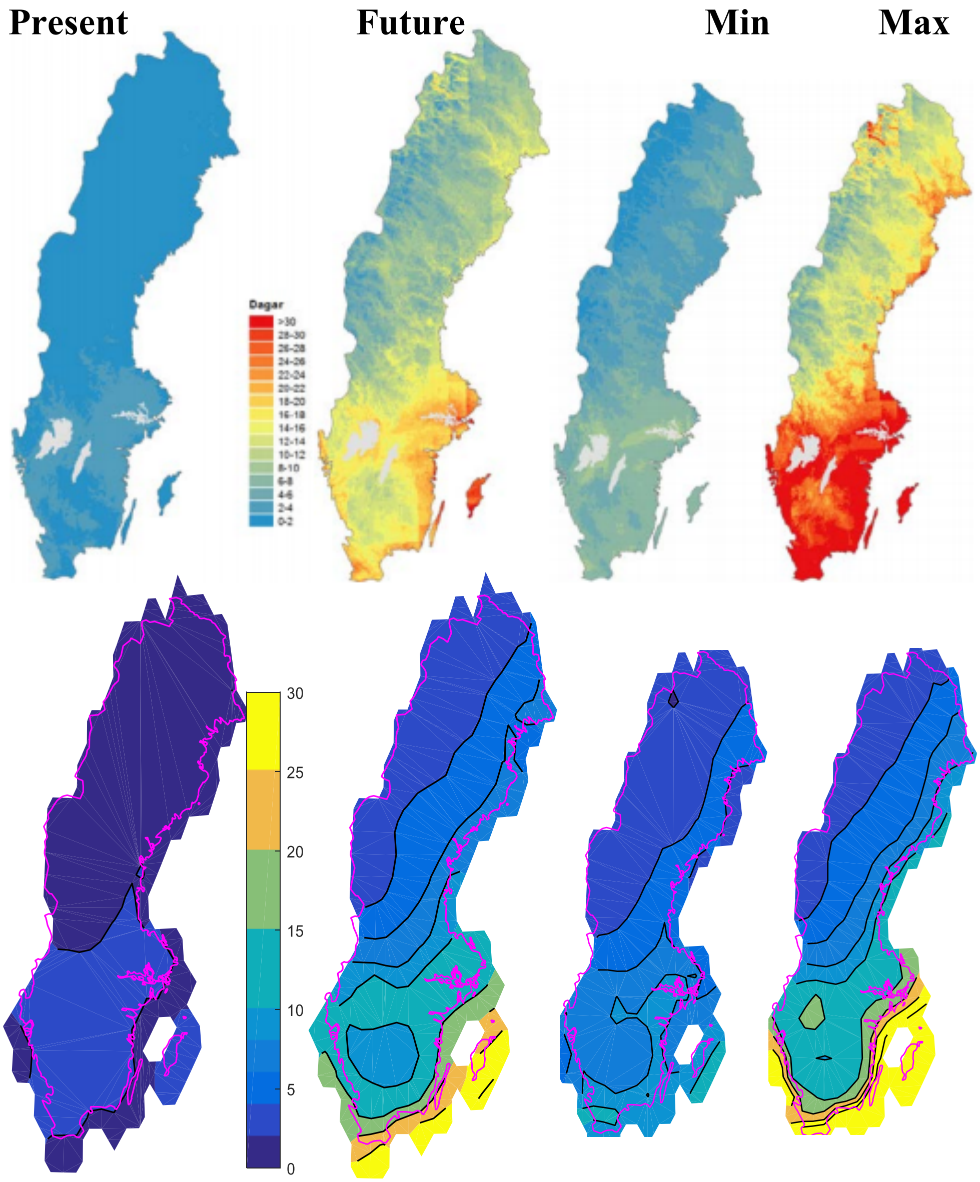

Figure 6.4: The SMHI (top) and d4PDF (bottom) present and future mean, minimum and maximum longest heat wave length (days) for the different models. The max and min maps show the model result with the maximum and minimum results for each grid point.

Yearly and seasonal precipitation

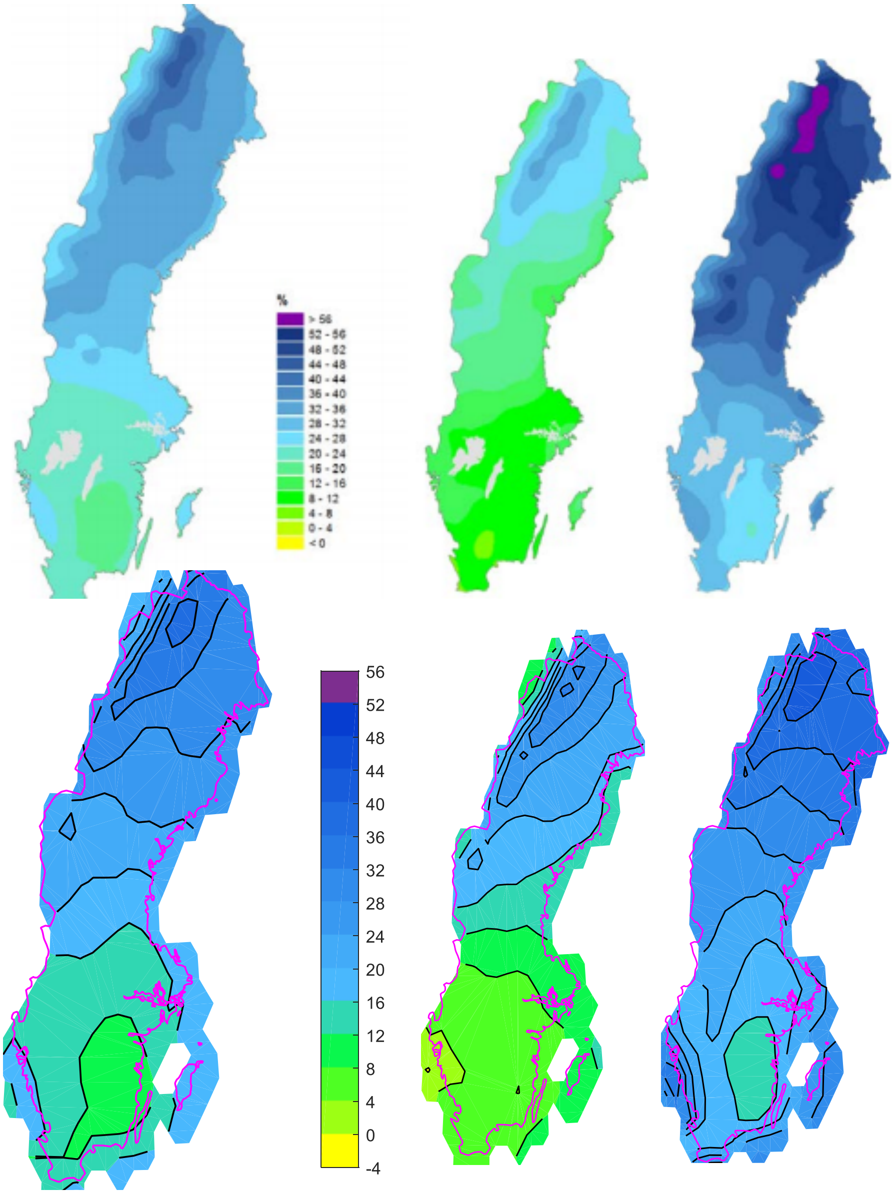

Mean **Min** **Max**

Figure 6.5: The change in average yearly precipitation for the SMHI (top) and d4PDF (bottom). Mean (left), min (center) and max (left). The max and min maps show the model result with the maximum and minimum results for each grid point.

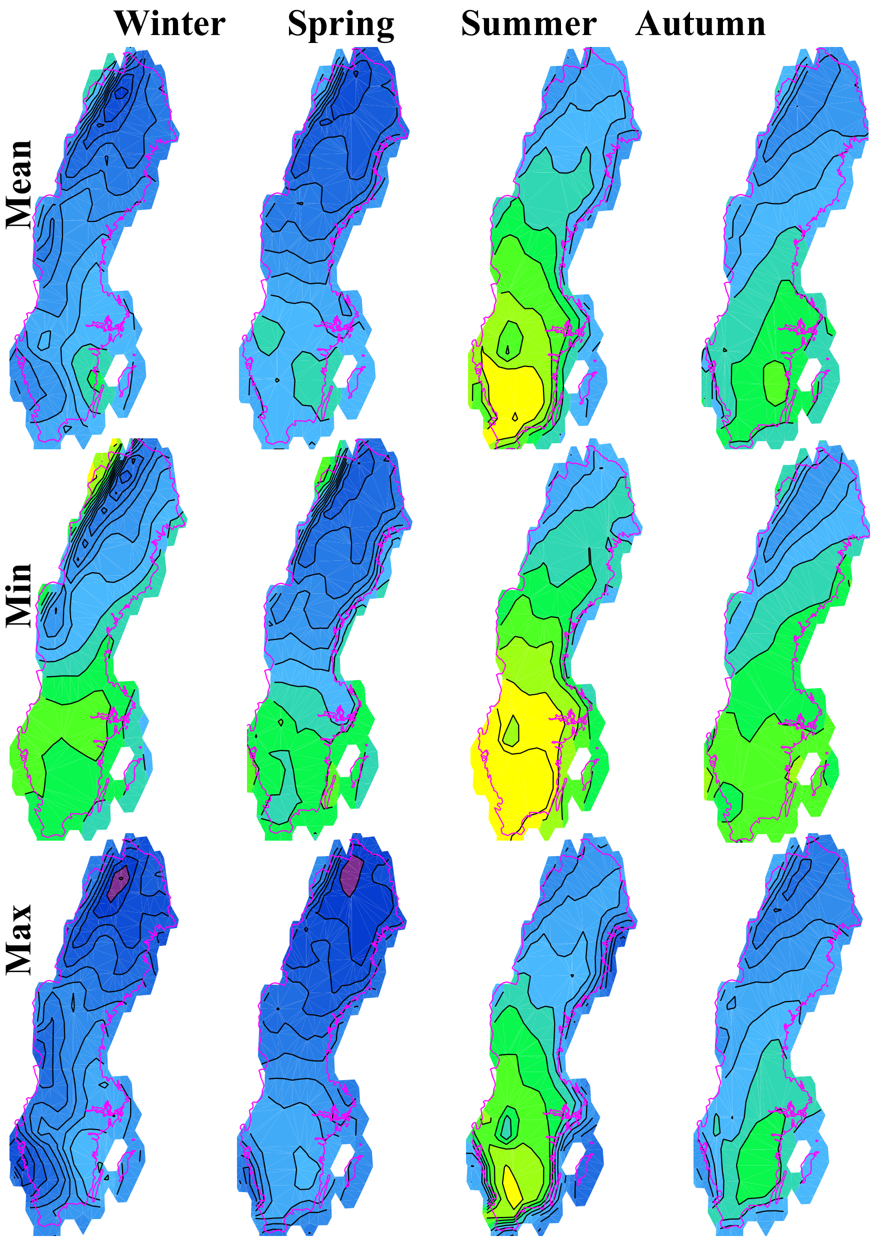

Figure 6.6: The d4PDF seasonal (left to right) precipitation change form 1961-1990 to the future climate. Mean (top), min (middle) and min (bottom). The max and min maps show the model result with the maximum and minimum results for each grid point.

Maximum daily precipitation

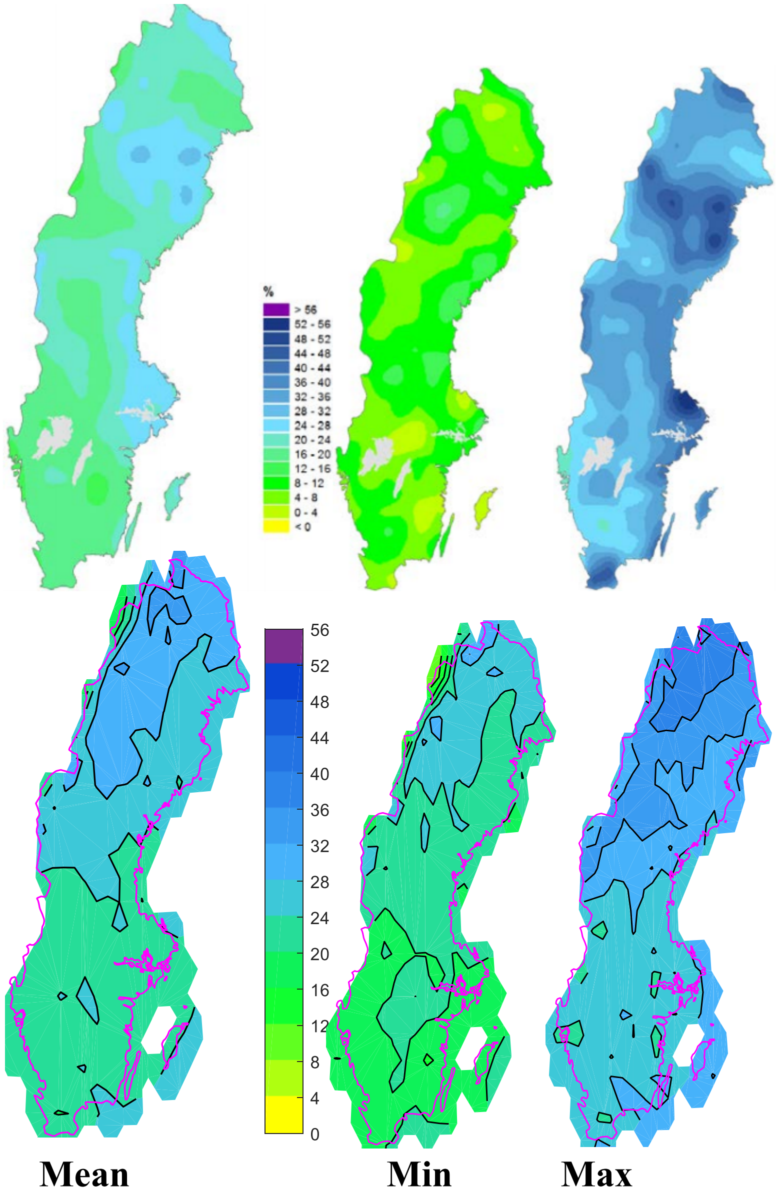

Figure 6.7: The change of the yearly average precipitation from 1961-1990 to 2069-2098 for the SMHI data (top) (Eklund et al., 2015) *and from 1961-1990 to the future data in the d4PDF (bottom). The max and min maps show the model result with the maximum and minimum results for each grid point.*